이학박사 학위논문

Salt-inducible kinase 1 regulates osteoblast differentiation via CRTC1

Salt-inducible kinase 1 의 CRTC1 을 통한 조골세포 분화 조절

2020 년 2 월

서울대학교 대학원
치의과학과 세포및발생생물학 전공
김민경

Salt-inducible kinase 1 regulates osteoblast differentiation via CRTC1

by

Min Kyung Kim

Advisor:

Prof. Hong-Hee Kim, Ph.D

A Thesis Submitted in Partial Fulfillment of the
Requirements for the Degree of Doctor of Philosophy

February, 2020

Division of Cell and Developmental Biology
Department of Dental Science, School of Dentistry
Seoul National University

ABSTRACT

Salt-inducible kinase 1 regulates osteoblast differentiation via CRTC1

Min Kyung Kim

Division of Cell and Developmental Biology

Department of Dental Science

Seoul National University

(Directed by Prof. Hong-Hee Kim, Ph.D)

A good understanding of the cellular and molecular mechanisms that regulate the various stages in bone metabolism is crucial for the development of therapeutic agents to prevent and treat bone diseases like osteoporosis. The present study demonstrates the function of salt-inducible kinase 1 (SIK1) in modulating osteogenesis. SIK1 expression was sharply downregulated among SIK isoforms during osteogenesis. Downregulation of SIK1 gene but not that of SIK2 or SIK3 in primary preosteoblasts promoted osteoblast differentiation and matrix mineralization. SIK1 also modulated the proliferation of osteoblastic precursor cells in osteogenic process. The catalytic activity of SIK1 was

required to regulate osteogenesis. SIK1 decreased CREB transcriptional activity for the expression of osteogenic genes like Id1 by phosphorylating CREB regulated transcription coactivator 1 (CRTC1). In addition, SIK1 knockout (KO) mice showed higher bone mass, osteoblast number, and bone formation parameters than WT, whereas the RANKL/OPG ratio and osteoclast number between KO and WT were not different. Moreover, bone morphogenic protein 2 (BMP2) reduced both SIK1 expression as well as catalytic activity by protein kinase A (PKA)–dependent manner. Taken together, these results demonstrate that SIK1 is a novel regulator of preosteoblast proliferation and osteoblastic differentiation and that the suppression of SIK1 is important for BMP2-mediated osteogenesis. Therefore, this study proposes that SIK1 is a possible therapeutic target for bone diseases.

Keywords: Bone, Osteoblast, SIK1, BMP2, CRTC1, CREB, Id1, PKA

Student Number: 2012-21832

This thesis contains the results of a study published in journal of "Cell Death and Disease".

CONTENTS

LIST OF FIGURE

LIST OF TABLES

LIST OF ABBREVIATIONS

MSCs	Mesenchymal stem cells
BMPs	Bone morphogenetic proteins
PTHrP	Parathyroid hormone-related peptide
RANK	Receptor activator of nuclear factor kB (NF-kB)
RANKL	RANK ligand
MNCs	Multinucleated cells
NFATc1	Nuclear factor of activated T cells c1
TRAP	Tartrate-resistant acid phosphatase
OPG	Osteoprotegerin
PKA	Protein kinase A
SIK	Salt-inducible kinase
AMPK	AMP-activated protein kinase
CRTC	CREB regulated transcription coactivator
HDAC	Histone deacetylase
CRE	cAMP responsive element.
Id	Inhibitors of DNA binding/differentiation
OSX	Osterix

ALP	Alkaline phosphatase
COL1A1	Collagen type I alpha 1
OCN	Osteocalcin
BSP	Bone sialoprotein
BMM	Bone marrow–derived monocyte/macrophages macrophage
SERMs	Selective estrogen receptor modulators
PKIs	Protein kinases inhibitor isoforms
KO	Knockout
WT	Wild-type
siRNA	Small interfering ribonucleic acid
ELISA	Enzyme-linked immunosorbent assay
ß-GP	Beta-glycerophosphate
AA	Ascorbic acid
µ-CT	Micro-computed tomography
ROI	Region of interest
Tb.BV/TV	Trabecular bone parameters; trabecular bone volume/total volume
Tb.Th	Trabecular thickness
Tb.N	Trabecular number
Tb.sp	Trabecular separation

Ct.BV/TV	Cortical BV/TV
Ct.Th	Cortical thickness
N.OB/B.pm	Osteoblast number per bone perimeter
OB.S/B.S	Osteoblast surface per bone surface
N.OC/B.Pm	Osteoclast number per bone perimeter
OC.S/BS	Osteoclast surface per bone surface
MS/BS	Mineralized surface per bone surface
MAR	Mineral apposition rate
BFR/BS	Bone formation rate per bone surface

1. INRODUCTION

Physiological bone remodeling and bone fracture repair throughout life as well as skeletal development require the accurate regulation of bone anabolism and catabolism. Osteogenesis is a multiple process involving osteoblast differentiation, synthesis of organic bone matrix called osteoid, and mineralization of osteoid. Osteoblast differentiation is accomplished through sequential steps including the commitment of mesenchymal stem cells to osteoprogenitors, proliferation of progenitor cells, early differentiation to immature osteoblasts, and differentiation to mature osteoblasts (Long, 2011; Rutkovskiy et al., 2016). These multiple steps are regulated by diverse groups of extracellular signals like bone morphogenic protein (BMP), Wnt, hedgehog, and parathyroid hormone-related peptide (PTHrP) via distinct or overlapping intracellular signaling pathways (Long, 2011) (Figure 1).

Osteoblastic cells formed and activated by osteogenic process control osteoclast differentiation. Receptor activator of nuclear factor κB ligand (RANKL; encoded by *Tnfrsf11b* gene) produced by mature osteoblasts or osteocytes coordinates osteoclast differentiation process including preosteoclast fusion to generate multinucleated cells (MNCs) and stimulates osteoclast resorptive activity via receptor activator of nuclear factor kB (NF-kB) (RANK) which is expressed on the surface of osteoclast precursors. During

differentiation, RANKL induces osteoclast-marker genes, such as *Acp5* which encodes the tartrate-resistant acid phosphatase (TRAP) and nuclear factor of activated T cells c1 (*Nfatc1*) (Takayanagi et al., 2002; Boyle et al., 2003). Furthermore, osteoblasts also express osteoprotegerin (OPG; encoded by *Tnfsf11* gene), a soluble decoy receptor of RANKL, which inhibits osteoclast differentiation and resorption activity by blocking RANKL/RANK binding (Boyle, Simonet et al., 2003). Therefore, cooperative actions between osteoblast and osteoclast continuously regulate bone homeostasis for healthy bone (Figure 2).

An imbalance between bone-formation by osteoblasts and bone resorption by osteoclasts in bone remodeling leads to skeletal metabolic diseases like osteoporosis which is characterized by a decrease in bone mineral density and alteration of the bone micro-structure which increase the risk of bone fracture (Chen and Sambrook, 2011). For several decades, osteoclast-targeted anti-resorptive drugs such as bisphosphonate and denosumab have been developed for the treatment of osteolytic disorders. Osteoclast-targeted drugs act to decrease osteoclast proliferation, maturation, and activity (Chen and Sambrook, 2011). More recently, osteoblast-targeted anabolic agents such as anti-sclerostin antibodies and teriparatide which act by enhancing

osteoblastic precursors proliferation, osteoblast maturation, and mature osteoblast survival were developed for osteoporosis and fracture treatments (Augustine and Horwitz, 2013; Corrado et al., 2017). However, these agents have revealed several side effects, placing limitations to clinical usage (Lotinun et al., 2002; Kennel and Drake, 2009; Augustine and Horwitz, 2013; Martinkovich et al., 2014; Zaheer et al., 2015; Meyer, 2019) (Table 1). Therefore, discovery of new therapeutic targets to increase anabolic activity without evoking unwanted effects is required.

The salt-inducible kinase (SIK) family belongs to the AMP-activated protein kinase (AMPK) family and contains three members (SIK1, SIK2, and SIK3) (Hardie and Carling, 1997). Although the three SIKs share structural domains and up- and downstream targets, SIK1 is different from SIK2 and SIK3 in their expression patterns and chromosome locations. While the levels of SIK2 and SIK3 are constitutive, SIK1 expression is regulated by external stimuli like high salt diet, adrenocorticotropin hormone, and glucagon (Wein et al., 2018). SIKs have been implicated in multiple processes including adrenal steroidogenesis, adipogenesis, pancreatic insulin secretion, hepatic gluconeogenesis, renal sodium transport, and neuronal survival (Takemori et al., 2003; Okamoto et al., 2004; Taub et al., 2010; Gallo and Iadecola, 2011;

Stewart et al., 2013; Kim et al., 2015). The activity of SIKs is stimulated by phosphorylation by LKB at a serine residue in the N-terminal kinase domain (Lizcano et al., 2004; Jaleel et al., 2005). In contrast, phosphorylation in the C-terminal domain by protein kinase A (PKA) inhibits SIK activity (Takemori et al., 2002; Henriksson et al., 2012). The best studied downstream targets of SIKs are CREB regulated transcription coactivator (CRTC; also called TORC) proteins and class IIa histone deacetylases (HDACs) (Katoh et al., 2006; Takemori et al., 2007; van der Linden et al., 2007; Li et al., 2009). Recently, TAB2 is revealed to be a target protein of SIK1 and SIK3 in Toll-like receptor signaling (Berdeaux et al., 2007; Yong Kim et al., 2013; Sanosaka et al., 2015; Lombardi et al., 2016). The phosphorylation of CRTCs by SIKs leads to binding with 14-3-3 as a cytosolic scaffold protein and subsequent cytoplasmic sequestration of CRTCs, preventing the nuclear action of CRTCs in potentiating CREB activity as a coactivator. Therefore, SIK negatively regulates CREB-mediated responses and PKA can negate SIK-mediated CREB inhibition (Katoh, Takemori et al., 2006; Sonntag et al., 2018) (Figure 3).

BMP family proteins elicit osteogenic responses by binding to the heteromeric complexes of type 1 and type 2 receptors. The activated receptor phosphorylates and thereby activates Smad1/5/9, which forms a complex with

Smad4. The Smad complex subsequently translocates to the nucleus. Smad stimulates Runx2 expression and cooperates with Runx2 for induction of other transcription factors involved in osteogenesis like the inhibitors of DNA binding/differentiation (*Ids*), *Sp7* which encodes the Osterix (OSX) and *Dlx* (Miyazono et al., 2005; Wu et al., 2016). Besides, BMP signaling induces the TAK1–MKK–MAPK axis, a non-Smad pathway, which facilitates the activation and also the expression of other osteogenic factors like Runx2 (Lee et al., 2002; Greenblatt et al., 2010; Ge et al., 2012). As a result, BMP signaling induces expression of genes needed for osteoblast function like alkaline phosphatase (*Alp*), collagen type I alpha 1 (*Col1a1*), and *Bglap,* a gene encoding osteocalcin (OCN) (Huang et al., 2007) (Figure 4).

Elevation in cAMP levels or PKA activity has been implicated in bone anabolic effects. In these responses, PKA has been thought to directly activate CREB by phosphorylating it (Datta and Abou-Samra, 2009). Activated CREB binds CRE on the promoter of osteogenic genes, such as *Id1*, bone sialoprotein (*Bsp*) and *Bglap*, and activates their transcription (Jongen et al., 1993; Yang and Gerstenfeld, 1996; Kondo et al., 1997). While the bone anabolic role of PKA has been mostly described for GPCR-stimulating signals like PTH (Datta and Abou-Samra, 2009; Vilardaga et al., 2011), BMP signaling has also been shown to utilize PKA in osteogenesis (Zhao et al., 2006; Viale-Bouroncle et al., 2015;

Zhang et al., 2015). As yet whether BMPs regulate cAMP levels is to be addressed, some studies have shown that PKA activation can be induced by BMPs via downregulation of protein kinase inhibitor γ (PKAγ) in dental follicle cells, mesenchymal stem cells, and C2C12 cells during osteogenic differentiation (Zhao, Yang et al., 2006; Viale-Bouroncle, Klingelhoffer et al., 2015; Zhang, Li et al., 2015) (Figure 5).

Several studies involving the regulation of SIKs by PKA and the bone anabolic role of PKA pathway may suggest a crosstalk between these kinases in bone development and metabolism. Indeed, SIK3 knock-out mice showed severe inhibition of chondrocyte hypertrophy (Sasagawa et al., 2012). In addition, SIK2 and SIK3, highly expressed in osteocytes, were shown to act as negative regulators in PTH-stimulated bone formation by suppressing expression of sclerostin, a Wnt inhibitor (Wein et al., 2016). However, the role of SIK1 in the skeletal bone system has not been investigated. This study shows that SIK1 regulates bone metabolism by modulating preosteoblast proliferation and osteoblast differentiation without affecting osteoclasts. SIK1 suppressed osteogenesis by inhibiting the CRTC1/CREB/Id1 pathway in primary preosteoblasts. SIK1 knock-out mice displayed higher bone mass and osteoblast activity compared to wild type mice. These results demonstrate that SIK1 plays a key role in maintaining bone homeostasis by regulating osteoblast

differentiation.

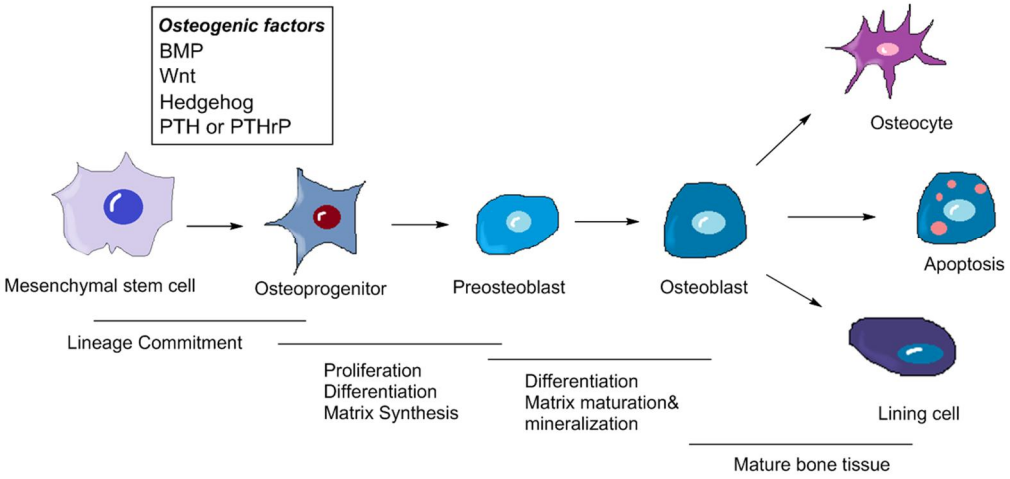

Figure 1. The sequence of osteoblast differentiation from stem cells. Osteoblasts differentiate from mesenchymal stem cells in sequential order of distinct events, which are governed by various signaling molecules like BMP, Wnt, hedgehog, PTH or PTHrP.

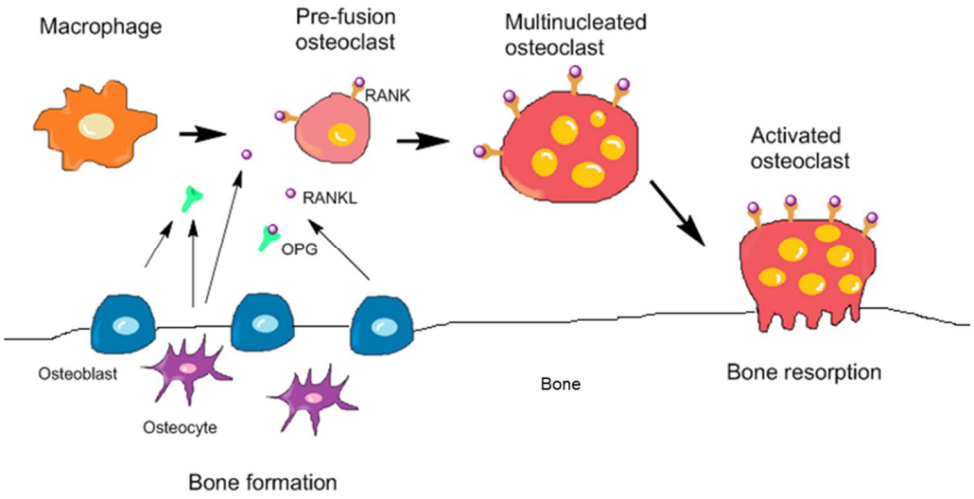

Figure 2. The regulation of osteoclast differentiation by osteoblastic cells in bone metabolism. Osteoblastic lineage cells differentiated from MSC produce RANKL and OPG, which regulate osteoclast differentiation. The binding of RANKL to its receptor RANK expressed on bone marrow-derived macrophages (BMMs), OC precursors, initiate osteoclast differentiation. OPG can antagonize binding of RANKL to RANK, which inhibits osteoclast differentiation. Thereby, the RANKL/OPG ratio determines osteoclastogenic potential.

Class	Mechanism	Side effects
Bisphosphonates (Alendronate, Ibandronate, Risedronate, and Zoledronic acid)	Inhibits action of osteoclasts which resorb bone, thereby osteoblasts can act more bone formation than destruction by osteoclast	Nausea, hypocalcemia, esophageal irritation, skeletal pain, osteonecrosis, and suppression of bone turnover (Kennel and Drake, 2009).
Denosumab (monoclonal antibodies against RANKL)	A human monoclonal antibody binding RANKL. Decreases the formation and activity of osteoclasts	Atypical femur fractures (AFF), osteonecrosis of the jaw (ONJ), severe symptomatic hypocalcemia (SSH), and anaphylaxis (Zaheer, LeBoff et al., 2015)
SERMs (selective estrogen receptor modulators)	Mimics the effects of estrogen and reverses the destruction of bone by menopause.	Hot flashes, fatigue, nausea, fatigue, headache, backpain, and dyspnea (Martinkovich, Shah et al., 2014)
Parathyroid hormone (Teriparatide)	Increases the activity of bone formation by osteoblasts	Hypercalcemia, headache, nausea and skeletal abnormalities associated with hyperparathyroidism (Lotinun, Sibonga et al., 2002)

Evenity (monoclonal antibodies against Sclerostin)	Blocks the effects of the protein sclerostin and increases new bone formation. Should not be used in patients who have had a heart attack or stroke within the previous year.	Heart attack, stroke, and cardiovascular death (Meyer, 2019)

Table 1. Bone anabolic and anti-resorptive reagents used for therapy of osteoporosis.

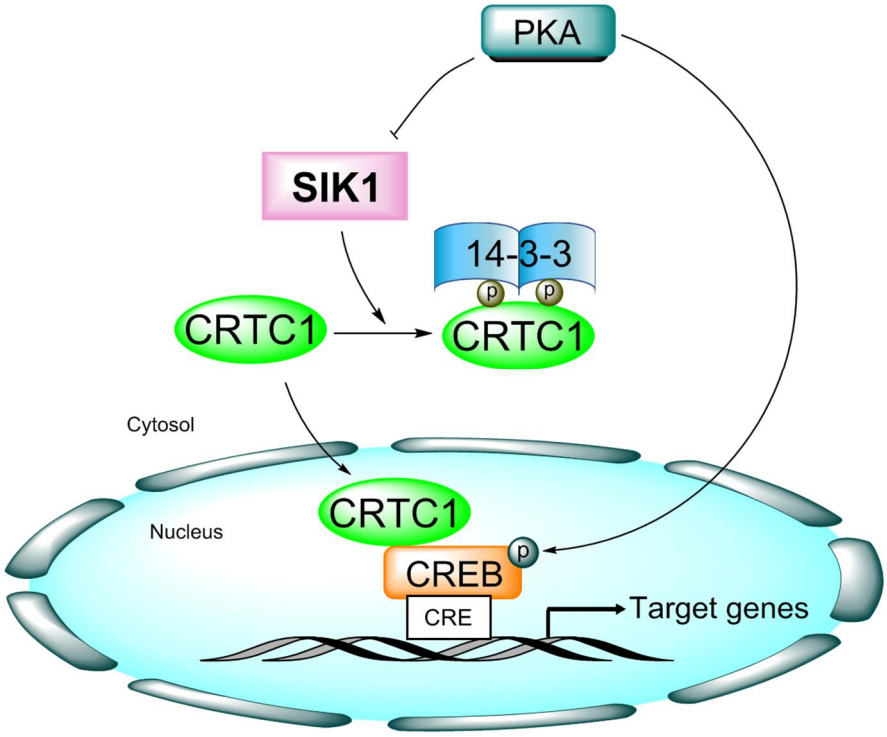

Figure 3. SIK regulates CREB activity via its target CRTC. SIK

phosphorylates and prevents translocation of CRTC into the nucleus, which inactivates CRTC which is a CREB-specific co-activator. As a result, inactive CRTC by SIK1 decreases CREB transcriptional activity and regulates target gene expression at promoters containing CREs. Under condition of PKA activation, SIK1 activity is inhibited, and dephosphorylated CRTC undergoes nuclear translocation. Thereby, CRTC promotes CREB activity and thereby induction of CREB target genes in a CREB phosphorylation-independent manner.

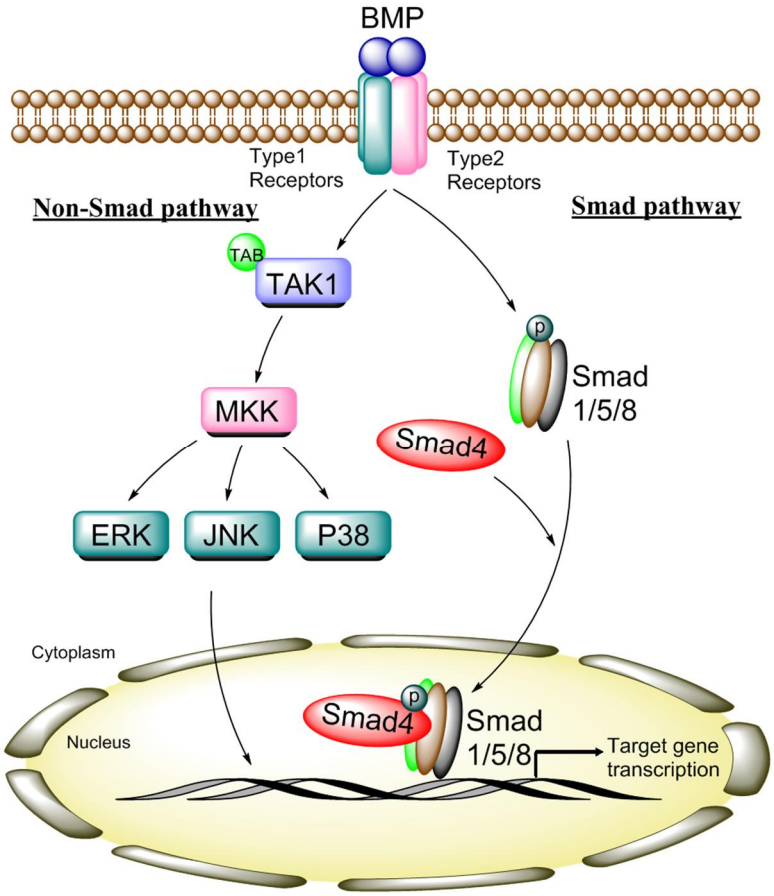

Figure 4. Non-Smad- and Smad-dependent BMP signaling pathways. Binding of BMP to a complex of type I and type II receptors elicits intracellular signaling through the non-Smad and Smad pathways. The Smad 1/5/8 complex binds to Smad4 and they translocate into the nucleus, thereby the complex associates transcriptional co-activators or co-repressors to regulate target genes. In non-canonical Smad signaling, the binding of receptor complex to ligand triggers a non-Smad pathway, which involves TAK1-MKK-MAPK axis.

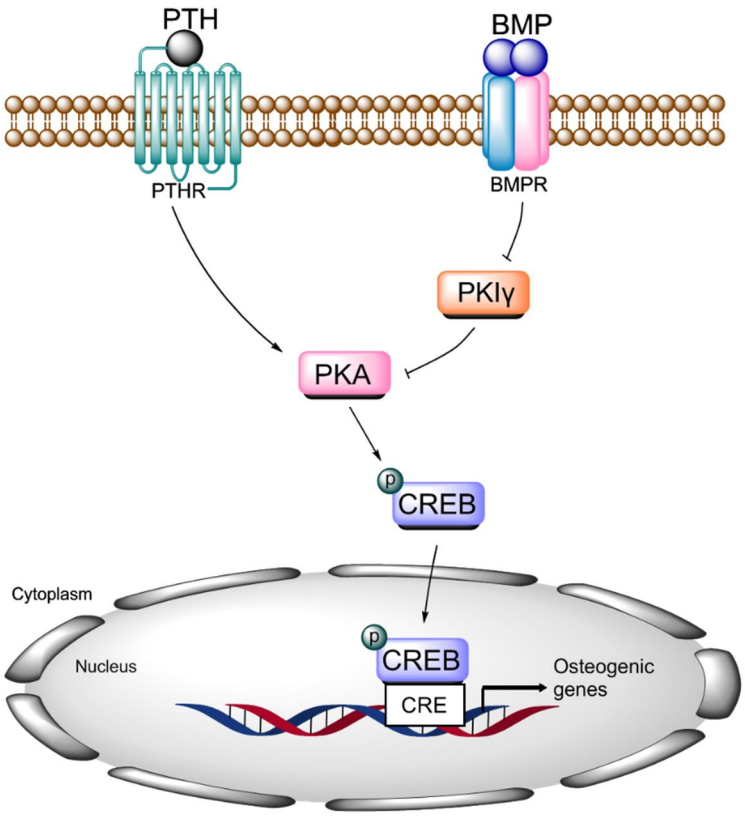

Figure 5. A cross-talk between cAMP-PKA and BMP signaling pathways. PKA activated in response to PTH directly induces CREB phosphorylation. Phosphorlyated CREB binds CRE on the promoter of osteogenic genes and promotes their transcription. In addition, BMP signaling utilizes PKA in osteogenesis by decreasing the transcription of PKIγ, one of PKA inihibitor.

2. MATERIALS AND METHODS

2.1. Animals

SIK1 knockout (KO) mice (C57BL/6) were previously described (Kim, Park et al., 2015). All experimental procedures were approved by the Institutional Animal Care and Use Committee of Seoul National University. Mice were housed in the SPF animal facility with a 12-hour day-night cycle. Neonatal ICR mice for the isolation of osteoblast precursors (preosteoblasts) and the experiments of *ex vivo* bone cultures were purchased from OrientBio (Seongnam, Korea).

2.2. Reagents

Recombinant human BMP2, M-CSF, and RANKL were purchased from PeproTech (Rocky Hill, NJ, USA). Phospho-specific (Ser151) and pan-CRTC1 antibodies were purchased from Cell Signaling Technology (Danvers, MA, USA). HG-9-91-01 was purchased from MedChemExpress (Princeton, NJ, USA). Antibodies against SIK1, Id1, Lamin B, and α-tubulin, were obtained from Santa Cruz Biotechnology (Santa Cruz, CA, USA). OCN antibody was acquired from Abcam (Cambridge, UK). Anti-β-actin and anti-HA were acquired from Sigma-Aldrich (St. Louis, MO, USA). HRP Anti-Rabbit IgG (Peroxidase) Polymer Detection Kit was purchased from Vector Laboratories

(Burlingame, CA, USA). Additionally, an alkaline phosphatase (ALP) assay kit was purchased from Takara Bio Inc. (Ohtsu, Japan), while an ALP staining kit, tartrate-resistant acid phosphatase (TRAP) staining kit, β-glycerophosphate, and ascorbic acid were purchased from Sigma-Aldrich (St. Louis, MO, USA). Mouse RANKL and OPG ELISA kits were purchased from R&D Systems (Minneapolis, MN, USA). pcDNA3-SIK1-HA, pcDNA3-SIK1-FLAG, and pcDNA3-SIK1-T182A-FLAG plasmids were as previously described(Kim, Park et al., 2015). pGL-Id1 (-1231/+88) plasmid was provided by Dr. Korchynskyi (National Academy of Sciences in Ukraine)(Korchynskyi and ten Dijke, 2002). siRNA oligonucleotides for control, SIK1, SIK2, SIK3, or CRTC1 were purchased from Thermo Fisher Scientific (Waltham, MA, USA).

2.3. Osteoblast differentiation

Primary preosteoblasts were prepared from calvarae of neonatal mice as described previously (Chen and Long, 2015; Kim et al., 2017). For the induction of osteogenesis, preosteoblasts were seeded at 3.5 x 10^4 per well in 48-well plates or 3.5 x 10^5 per well in 6-well plates in α-MEM containing 10% FBS. On the next day, the medium was changed to an osteogenic medium containing 10 mM of β-glycerophosphate (β-GP) and 100 μg/mL of ascorbic acid (AA) in α-MEM/10% FBS. Alternatively, cells were cultured with

recombinant hBMP2 (150 ng/mL), a well-characerized osteogenic factor (Katagiri et al., 1990; Traianedes et al., 1998; Tare et al., 2002), in α-MEM/10% FBS. For osteoblastic differentiation of the C2C12 myoblastic cell line, cells were seeded at 0.7 x 10^4 per well in 48-well plates or 0.7 x 10^5 per well in 6-well plates in DMEM/10% FBS and the medium was changed on the next day to the one containing hBMP2 (150 ng/mL). To qualitatively evaluate the differentiation extent, cells were stained for ALP activity. Alternatively, cells were lysed and cell lysates were subjected to quantitative ALP activity assay. Matrix mineralization was assessed by staining the cultures with Alizarin Red S. In quantitative experiments, the stained cells were incubated with 100 mM of cetylpyridium chloride for two hours at 37˚C and the extracts were subsequently subjected to spectrophotometry at 415 nm.

2.4. *In vitro* gene knockdown

Preosteoblasts were seeded at 3.5 x 10^4 per well in 48-well plates or 3.5 x 10^5 per well in 6- well plates and C2C12 were seeded at 0.7 x 10^4 per well in 48-well plates or 0.7 x 10^5 per well in 6-well plates. After culturing overnight, Small interfering ribonucleic acid (siRNA) oligonucleotides (40 nM) were transfected into cells using HiPerFect (Qiagen, Venlo, Netherlands) following the manufacturer's protocol. In double knockdown experiments, the

concentration of each siRNA was 25 nM. On the following day, the cells received the osteogenic medium or BMP2 for differentiation. The expression level of protein or mRNA was determined at two days after transfection. The sequences of customized oligonucleotides are shown in Table 2.

2.5. *In vitro* gene overexpression

Preosteoblasts were seeded at 5 x 10^4 per well in 48-well plates or 5 x 10^5 per well in 6-well plates, and C2C12 were seeded at 1 x 10^4 per well in 48-well plates or 1 x 10^5 per well in 6- well plates. After culturing overnight, cells were transfected with pcDNA3 (EV), pcDNA3-SIK1-WT, or pcDNA3-SIK1-T182A constructs utilizing PolyFect (Qiagen, Venlo, Netherlands) according to the manufacturer's instructions. On the next day, the cells were treated with the osteogenic medium or BMP2 for differentiation.

2.6. Luciferase reporter assay

To assay the activity of gene promoter, C2C12 cells were seeded at 1 x 10^4 per well in 48-well plates. Cells were transfected on the next day with CRE-Luc or Id1-Luc reporter construct using PolyFect (Qiagen, Venlo, Netherlands) according to the manufacturer's instructions. After incubation for 12 hours,

cells were stimulated with hBMP2 (150 ng/mL) for 12 hours. The cells were lysed with the Glo lysis buffer (Promega Corp., Madison, WI, USA) and cell lysates were subjected to luciferase assay with the Bright-Glo luciferase assay kit and GloMax96 luminometer (Promega Corp., Madison, WI, USA). Luciferase activity was normalized to the protein concentration of each sample.

2.7. Cell proliferation assay

Calvarial preosteoblasts (1 x 10^4) or C2C12 (0.25x 10^4) cells were seeded onto 96-well plates. From the next day (day 0) cell were cultured in osteogenic conditions with the medium changed every day. Cell proliferation assay was performed daily with either the BrdU cell proliferation assay kit (Millipore Corp., MA USA) or the CCK-8 kit (Dogindo Molecular Technology, Japan), following the manufacturers' protocols.

2.8. Osteoclast differentiation

BMMs were prepared as previously described (Kim et al., 2012). In brief, bone marrow cells were isolated from the tibiae and femurs of female five-week-old littermate WT or SIK1 KO mice and cultured in α-MEM containing 10% FBS overnight on culture dishes. Nonadherent cells were collected and cultured in

the presence of M-CSF (30 ng/mL) for three days on Petri dishes. Attached cells (BMMs) were harvested and seeded at 3.5 x 10^4 per well in 48-well plates or 3.5 x 10^5 per well in 6-well plates with M-CSF (30 ng/mL). From the following day, cells were cultured with M-CSF (30 ng/mL) and RANKL (150 ng/mL) for four days to induce osteoclast differentiation. TRAP staining was performed in accordance with the manufacturer's instructions.

2.9. Real-time PCR analysis

Analyses of mRNA expression levels by real-time PCR were carried out as previously described (Kim, Prasad et al., 2012). The primers used for real-time PCR analyses are listed in Table 3.

2.10. Western blotting

Cells were lysed with RIPA buffer (50 mM Tris-HCl, pH: 8.0, 150 mM NaCl, 0.1% SDS, 1% NP40, 0.5% sodium deoxycholate, 0.5 mM PMSF, proteinase inhibitor cocktail, 1 mM Na_3VO_4, and 1 mM NaF). Following protein quantification with the DC Protein Assay Kit (Bio-Rad Laboratories, Hercules, CA, USA), equal amounts of lysates were subjected to Western blotting as described previously (Yoon et al., 2011).

2.11. Extraction of cytoplasmic and nuclear proteins

Cytoplasmic and nuclear fraction proteins were prepared using the NE-PER Nuclear and Cytoplasmic Extraction Kit (Thermo Fisher Scientific, Waltham, MA, USA) according to the manufacturer's instructions. In brief, cells were washed with cold PBS twice and treated with the cytoplasmic lysis buffer. After centrifugation, the supernatant was transferred to a new tube as cytoplasmic protein and the pellet was washed and treated with the nuclear lysis buffer. After centrifugation, nuclear protein was obtained from the supernatant.

2.12. Immunocytochemistry

To detect the protein expression of SIK1 by confocal microscopy, cells cultured on cover glasses were fixed with 3.7% formaldehyde and permeabilized with 0.1% Triton X-100. After blocking with PBS containing 1% BSA, cells were incubated overnight with anti-SIK1 antibody at 4˚C. Prior to incubation with Cy3-conjugated secondary antibody. Cover glasses were mounted with a mounting medium containing DAPI (Vector Laboratories, Burlingame, CA, USA) and observed under a confocal microscope (LSM700; Carl Zeiss AG, Oberkochen, Germany).

2.13. Calvarial organ culture and immunohistochemistry

Calvarial organ cultures were performed as previously described with slight modifications (Oh et al., 2012). In brief, calvariae from four-day-old ICR mice (n = 9 per group) were cultured in IVF organ culture dishes (Corning Inc., Corning, NY, USA) in BGJB medium (Thermo Fisher Scientific, Waltham, MA, USA). The organs were transfected with the control or SIK1 siRNA (600 nM) and cultured for seven days with BMP2 (200 ng/mL). The medium was changed every two days. For analyzing mRNA, calvariae were grounded after freezing and total RNA was isolated with Trizol (Thermo Fisher Scientific, Waltham, MA, USA). For immunohistochemistry, calvariae were fixed in 4% paraformaldehyde for overnight and decalcified with 12% EDTA (pH 7.4) for 14 days before embedding in paraffin. Coronal sections prepared in 5-μm thickness were deparaffinized in xylene and rehydrated in ethanol. The sections were heated in 10 mM sodium citrate (pH 6.0) for 20 minutes for antigen retrieval. To block endogenous peroxidase activity, the sections were incubated for 20 minutes in 3% H_2O_2 in methanol. Then, the sections were incubated overnight with anti-OCN at 4˚C. Following incubation with a HRP polymer-conjugated secondary antibody for 30 minutes, horseradish peroxidase activity was visualized using the DAB Peroxidase Substrate Kit (Vector Laboratories,

Burlingame, CA, USA). The sections were counterstained with Gill's hematoxylin (Vector Laboratories). The stained images were captured with a camera-equipped microscope and OCN-positive cells on bone surfaces around the sagittal suture were scored.

2.14. Calcein double labeling

Female wildtype (WT) or SIK1 KO mice (eight weeks old; n = 9 per group) were injected intraperitoneally with 20 mg/kg of calcein (Sigma-Aldrich, St. Louis, MO, USA) dissolved in 2% sodium bicarbonate at one and seven days before sacrifice on day 10. Femurs were fixed in 4% paraformaldehyde and undecalcified bones were embedded in methyl methacrylate. Sliced sections (5 μm) were observed under a confocal microscope (LSM700; Carl Zeiss AG, Oberkochen, Germany) and the distance between the calcein deposited bands was measured.

2.15. μCT analysis and histomorphometry

Femurs of 10-week-old littermate WT and SIK1 homozygous KO female mice (n = 9 per group) and male mice (n = 5 per group) were analyzed using the SkyScan 1172 μCT scanner (70 kV, 141 μA, 6.92 pixel size; Skyscan,

Aartselaar, Belgium). Trabecular bones were analyzed in 1-mm thickness area of distal femurs, starting from 1-mm below the growth plate and cortical bones were measured in the 1-mm thickness region starting from 3.5-mm below the growth plate where trabeculae were absent the thresholds were minimum 75 and maximum 255. Three-dimensional images were reconstituted using CT-volume software (Skyscan). For histological study, the fixed femurs were decalcified and embedded in paraffin. Serial sections (5 μm) of paraffin blocks were subjected to Goldner's trichrome and TRAP staining. The images were captured by bright field microscopy and histomorphometric analysis was carried out with the Osteomeasure software program (Osteometrics, Inc., Decatur, CA, USA) as described previously (Chang et al., 2008). In the sections stained with Goldner's trichrome, osteoblast parameters were analyzed by measuring the values of area and surface perimeter of trabecular bones and the number of osteoblastic cells lining trabecular bone surface in a region below the growth plate with the same region of interest (ROI). To determine osteoclast parameters, the values of area and surface perimeters of trabecular bones and the number of TRAP-positive cells on bone surfaces were measured in a region below the growth plate with the same ROI.

2.16. Statistical analysis

All quantitative data are shown as the means ± SDs. All in vitro experiments were repeated three to five times. The *ex vivo* calvaria culture experiment was repeated twice and the *in vivo* analysis of femurs was performed once for each sex. The significance of differences between two groups was determined using a Student's *t*-test. The comparison of multiple groups was carried out by using a one-way analysis of variance. A *P* value of less than 0.05 was considered to be significant.

genes	oligonucleotides sequences
Sik1	5’-CCA CAG CUC ACU UCA GCC CUU AUU A
	3’-UAA UAA GGG CUG AAG UGA GCU GUG G
Sik2	5’-AGA AGC AGU CUC AGC UGC AAG CAU A
	3’-UAU GCU UGC AGC UGA GAC UGC UUC U
Sik3	5’-CCA CAU GCU GGU GUU AGA UCC AAA U
	3’-AUU UGG AUC UAA CAC CAG CAU GUG G
Crtc1	5’-GGA GAG UCA CCA CCG AGC CUC UCU A
	3’-UAG AGA GGC UCG GUG GUG ACU CUC C

Table 2. Sequences of siRNA oligonucleotides

genes	primer sequences	
Hprt	F	CCT AAG ATG AGC GCA AGT TGA A
	R	CCA CAG GGA CTA GAA CAC CTG CTA A
Sik1	F	AGA AAT TCT CCC GTG TGA CC
	R	CCA CTG CAG TTG GTA TCC AG
Sik2	F	TCC AAG ACC TTT CGA GCA GT
	R	GGA AGA GTC GCT TCT GTT GG
Sik3	F	TGC TGG GAA CTG TGA GTC AG
	R	TGT TCT GGA TCG TGT GGT GT
Crtc1	F	CAG GCA GGC CAA TGC TCT GT
	R	CGC TCA GAC CCA TCA TGG CA
Alp	F	GAC TGG TAC TCG GAT AAC GA
	R	TGC GGT TCC AGA CAT AGT GG
Sp7	F	TCT ACC TGC GAC TGC CCC AA
	R	ATG CGA AGC CTT GCC GTA CA
Bglap	F	CCG GGA GCA GTG TGA GCT TA
	R	TAG ATG CGT TTG TAG GCG GTC
Id1	F	TCC TGC AGC ATG TAA TCG AC
	R	GTG GTC CCG ACT TCA GAC TC
Tnfsf11	F	TGG AAG GCT CAT GGT TGG AT
	R	CAT TGA TGG TGA GGT GTG CAA
Acp5	F	CGA CCA TTG TTA GCC ACA TAC G
	R	TCG TCC TGA AGA TAC TGC AGG TT
Col1a1	F	GCA TGG CCA AGA AGA CAT CC
	R	CCT CGG GTT TCC ACG TCT
Runx2	F	CGC ACG ACA ACC GCA CCA
	R	CAG CAC GGA GCA CAG GAA GTT

Table 3. Primer sequences for real-time PCR

3. RESULTS

3.1. SIK1 is selectively down-regulated during osteoblast differentiation

First, the expression patterns of SIK isoforms were examined during osteogenic process. Osteoblast precursors from mice calvariae were cultured with an osteogenic medium containing β-GP and AA and mRNA levels of SIKs were determined. The expression of *Sik1* mRNA was dramatically decreased in 2 days (Figure 6A). In contrast, the mRNA expression of *Sik2* and *Sik3* was decreased to a marginal degree only in a later stage of osteoblast differentiation (Figure 6A). Consistently, the level of SIK1 protein was evidently decreased during osteoblast differentiation (Figure 6B).

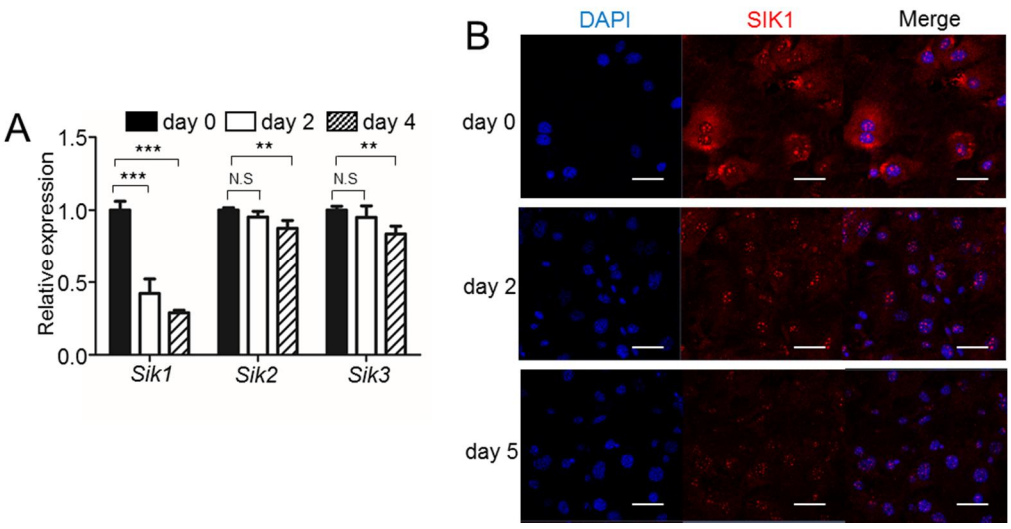

Figure 6. SIK1 was downregulated during osteoblast differentiation. (A, B) Primary preosteoblasts were treated with osteogenic medium containing ß-GP and AA. (A) The mRNA levels of SIK members were analyzed by real-time PCR. (B) After osteogenic culture, cells at Days 0, 2, and 5 were incubated with anti-SIK1 followed by Cy3-conjugated secondary antibody. Cells mounted with a mounting solution containing DAPI were observed under a confocal microscope. Scale bars, 50μm.

3.2. SIK1 deficiency enhances osteogenesis *in vitro*

To determine whether SIKs are involved in the regulation of osteogenesis, the gene expression level of each SIK member by RNA interference was downregulated in primary mouse precursor cells, and the transfected cells were cultured in osteogenic medium containing β-GP and AA. Specific gene knockdown was achieved for each SIK (Figure 7A). In SIK1 knockdown cells, we observed elevated levels of ALP staining, an osteoblast differentiation marker (Figure 7B). In contrast, SIK2 or SIK3 knockdown had little effect on ALP staining under the conditions in which the extents of knockdown efficiency were similar (Figure 7A and 7B), suggesting a specific role of SIK1 in controlling osteoblast differentiation. To gain further evidence for the function of SIK1 in osteogenesis, the cells knockdowned by SIK1 siRNA and cells lacking *Sik1* gene were utilized. In SIK1 knockdown cells, level of ALP activity measured by quantitative assay was also elevated (Figure 8A and 8B). The SIK1 deficiency enhanced matrix mineralization activity, as revealed by Alizarin Red staining (Figure 8C). The mRNA levels of osteogenic genes *Sp7*, *Alp*, and *Col1a1* were significantly increased by SIK1 siRNA

(Figure 9A). Intriguingly, mRNA expression of *Runx2* was not altered in SIK1 deficient cells, while Runx2 protein levels were increased (Figure 10A and 10B). SIK1 knockdown accelerated BMP2-induced osteoblastic differentiation of C2C12 cells (Figure 11). In addition, preosteoblasts from WT or of SIK1 KO mice were subjected to *in vitro* differentiation. Gene KO of *Sik1* did not affect the *Sik2* and *Sik3* expression levels (Figure 12). The ALP staining of osteogenic cultures of preosteoblasts showed greater differentiation in the SIK1 KO group versus in the WT group (Figure 13). The activity of matrix mineralization represented with Alizarin red staining also revealed higher level in SIK1 KO cells that WT cells (Figure 14). In line with these staining results, the expressions of *Id1*, *Sp7*, *Alp*, *Bglap*, and *Col1a1* were significantly elevated in SIK1 KO cells (Figure 15).

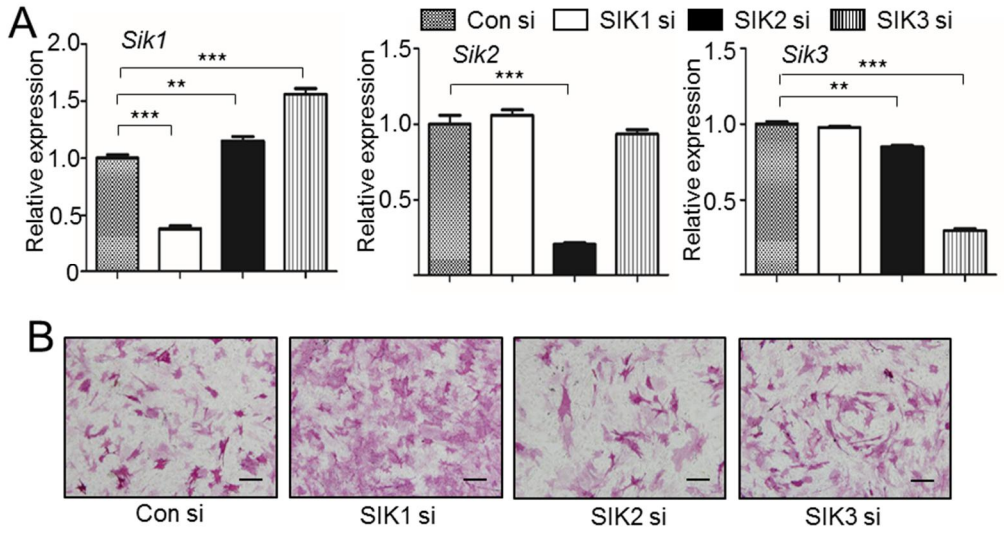

Figure 7. SIK1, not SIK2 and SIK3, regulates osteoblast differentiation. (A, B) Primary preosteoblasts were transfected with siRNA targeted to each SIK gene or control siRNA, then cultured with osteogenic medium. (A) The mRNA levels of *Sik1*, *Sik2*, and *Sik3* were determined by real-time PCR. (B) siRNA-transfected cells were cultured in osteogenic medium. Cells were stained for ALP activity at day 3. ***, $p < 0.001$; **, $p < 0.01$ versus control. t-test. Scale bars, 200 μm in B.

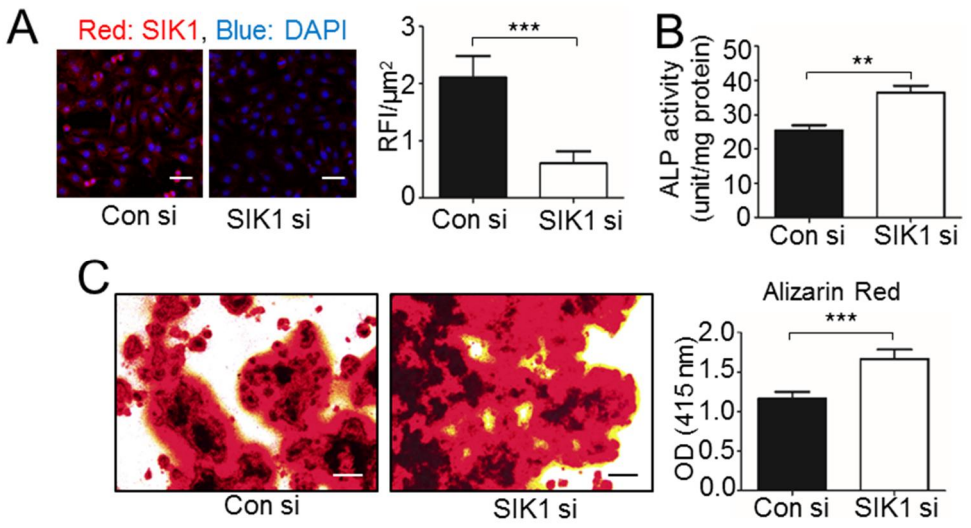

Figure 8. SIK1 knockdown increases osteoblast mineralization in mouse primary preosteoblasts. (A-C) Primary preosteoblasts were transfected with siRNA. (A) To quantify the extent of SIK1 knockdown at the protein level, cells were subjected to immunofluorescence microscopy. The fluorescence intensity of Cy3-labeled cells was analyzed by confocal microscopy. (B, C) cells transfected with siRNA were treated with osteogenic medium. (B) ALP activity was measured with cell lysates at day 3. (C) Matrix mineralization was evaluated by Alizarin Red staining at day 12, followed by stain extraction and

spectrophotometry. ***, $p < 0.001$; **, $p < 0.01$ verse control. Scale bars, 50 μm in A and 200 μm in C.

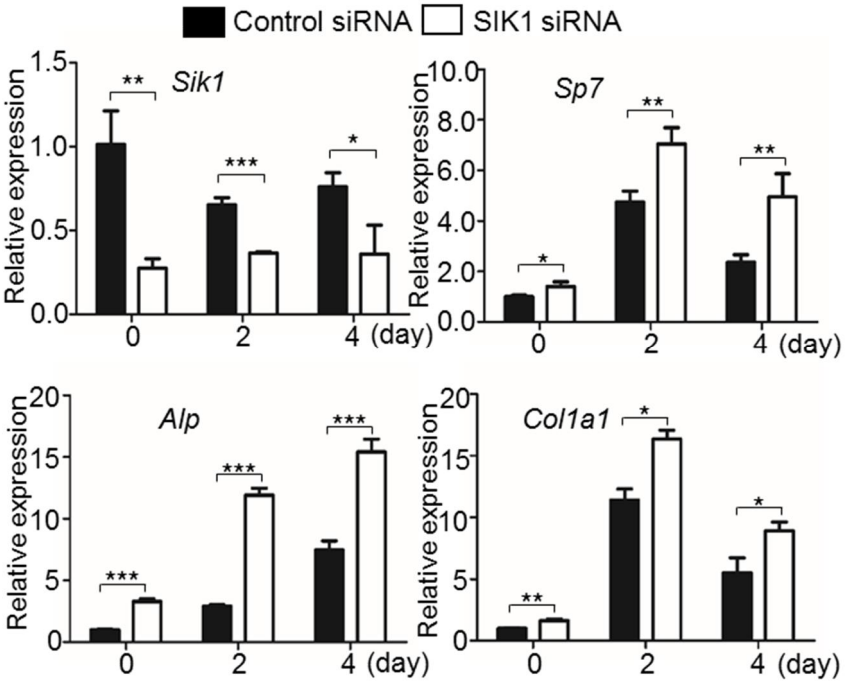

Figure 9. SIK1 deficiency enhances the expression levels of osteogenic genes. Primary preosteoblasts were transfected with SIK1 or control siRNA. Cells were cultured with osteogenic medium. The mRNA expression levels of *Sik1*, *Sp7*, *Alp*, and *Col1a1* were also analyzed by real-time PCR. ***, $p < 0.001$; **, $p < 0.01$; *, $p < 0.05$ versus control. t-test.

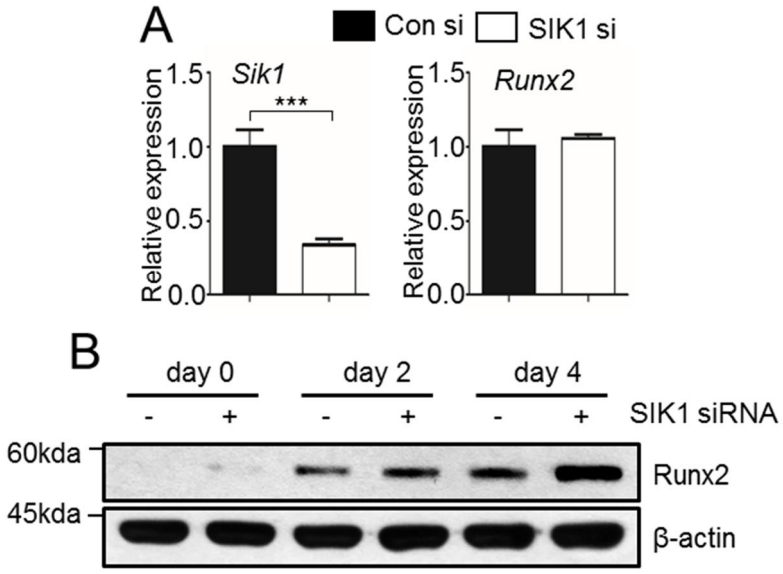

Figure 10. SIK1 knockdown increases the protein expression level of Runx2 not mRNA. (A, B) Primary preosteoblasts were transfected with siRNA and then cultured with osteogenic medium. (A) After 3 days of culture, *Runx2* mRNA levels were determined by real-time PCR. (B) The level of Runx2 protein was assessed at the indicated days by Western blotting. ***, $p < 0.001$ verse control.

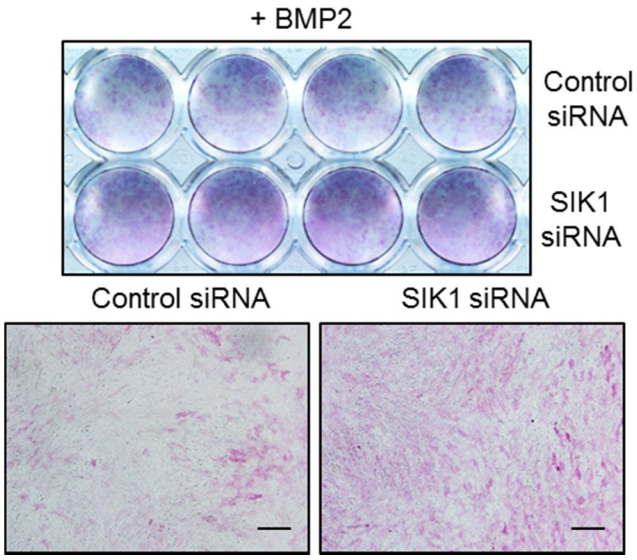

Figure 11. SIK1 knockdown enhances BMP2-induced osteoblastic differentiation of C2C12. C2C12 cells were transfected with targeted to SIK1 or control siRNA. Cells were then cultured in the presence of hBMP2 (150 ng/mL) for three days. Cells were stained for ALP activity. Scale bars, 200 μm.

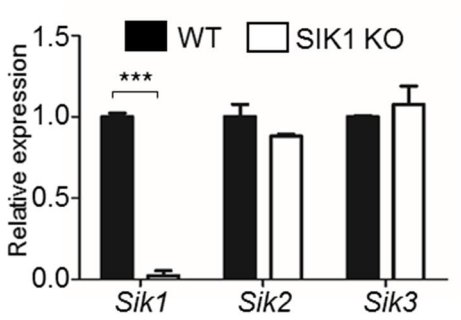

Figure 12. The expression of SIK isoforms in SIK1 KO cells *in vitro*. Calvarial preosteoblasts from WT and SIK1 KO mice were cultured. The relative mRNA levels of *Sik1*, *Sik2*, and *Sik3* were analyzed by real-time PCR. ***, $p < 0.001$ versus control. t-test.

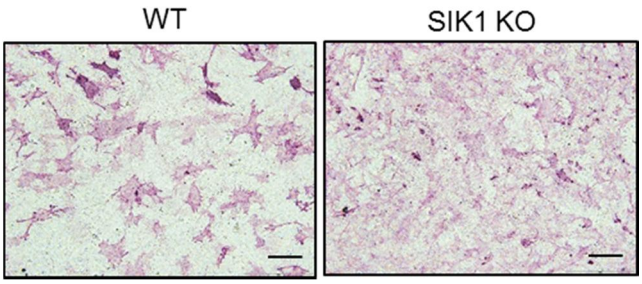

Figure 13. SIK1 KO enhances osteoblast differentiation *in vitro*. Primary preosteoblasts isolated from SIK1 KO or WT mice were cultured with osteogenic medium. Differentiated cells were subjected to ALP staining at day 3. Scale bars, 200 μm.

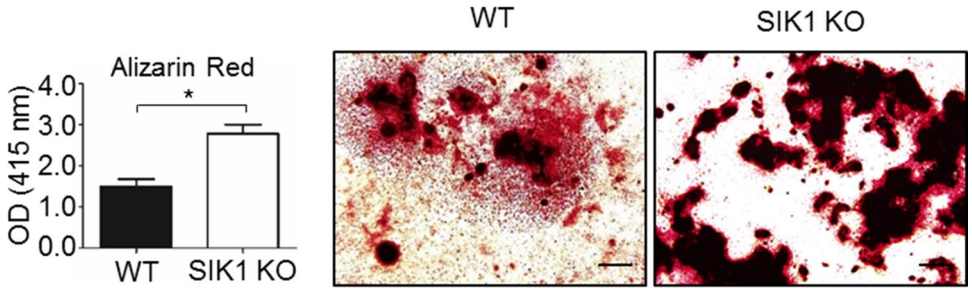

Figure 14. SIK1 KO cells increase matrix mineralization of osteoblast. Primary preosteoblasts isolated from SIK1 KO or WT mice were cultured with osteogenic medium. Matrix mineralization was assessed by Alizarin Red staining (Day 14) and the stain was quantified. *, $p < 0.05$ versus control. t-test. Scale bars, 200 μm.

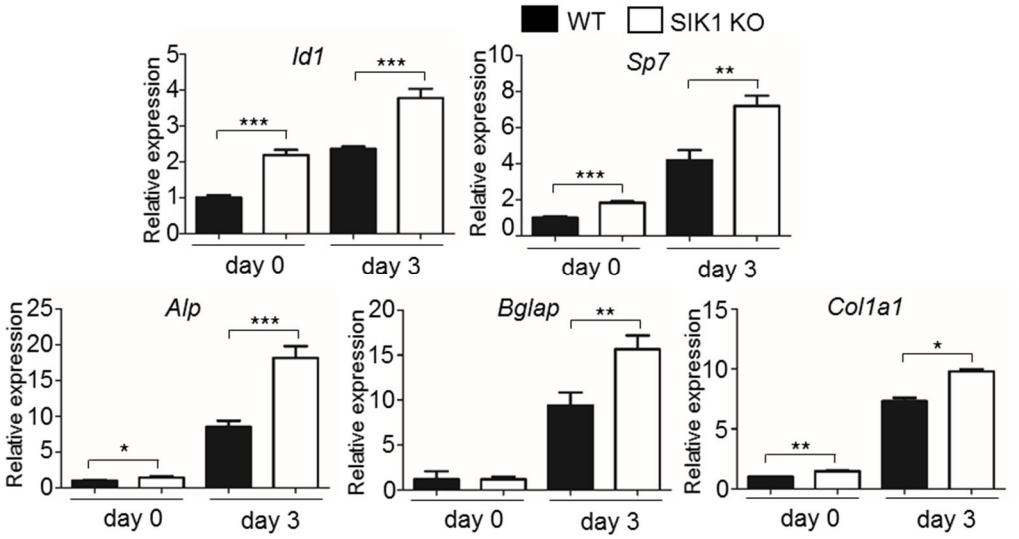

Figure 15. SIK1 KO cells enhance the expression levels of osteogenic marker genes. Primary preosteoblasts of SIK1 KO or WT mice were cultured with osteogenic medium for 3 days. The mRNA expression levels of *Id1*, *Sp7*, *Alp*, *Bglap*, and *Col1a1* at the indicated days were determined by real-time PCR. ***, $p < 0.001$; **, $p < 0.01$; *, $p < 0.05$ versus control. t-test.

3.3. SIK1 knockdown enhances osteogenesis *ex vivo*

Next, the osteogenic effect of SIK1 knockdown in bone tissues *ex vivo* was evaluated. Mice calvariae were cultured in organ culture dishes in the presence of control siRNA or SIK1 siRNA together with BMP2. ALP staining of calvariae showed a stronger activity in the SIK1 knockdown group than in the control knockdown group (Figure 16A). Analyses of calvariae mRNA confirmed an elevation in *Alp* level and a reduction in *Sik1* expression by the *ex vivo* treatment of SIK1 siRNA (Figure 16B). In histological studies, decalcified sections of calvariae were stained with anti-OCN antibody to label osteoblasts. The number of OCN^+ osteoblasts was increased by SIK1 siRNA (Figure 17). Collectively, these results suggest that SIK1 negatively regulates osteoblast differentiation and matrix mineralization *in vitro* and *ex vivo*.

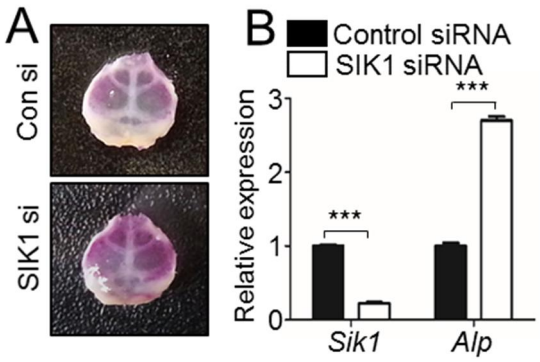

Figure 16. SIK1 knockdown increases the expression level of ALP mRNA and the activity of ALP staining in calvarial bone *ex vivo*. (A-B) Calvariae from four-day-old mice were transfected with control siRNA or SIK1 siRNA and cultured with hBMP2 (200 ng/mL) for seven days ex vivo. Calvariae were stained for ALP (A) or analyzed for mRNA levels of *Sik1* and *Alp* by real-time PCR (B). ***, $p < 0.001$ versus control. t-test.

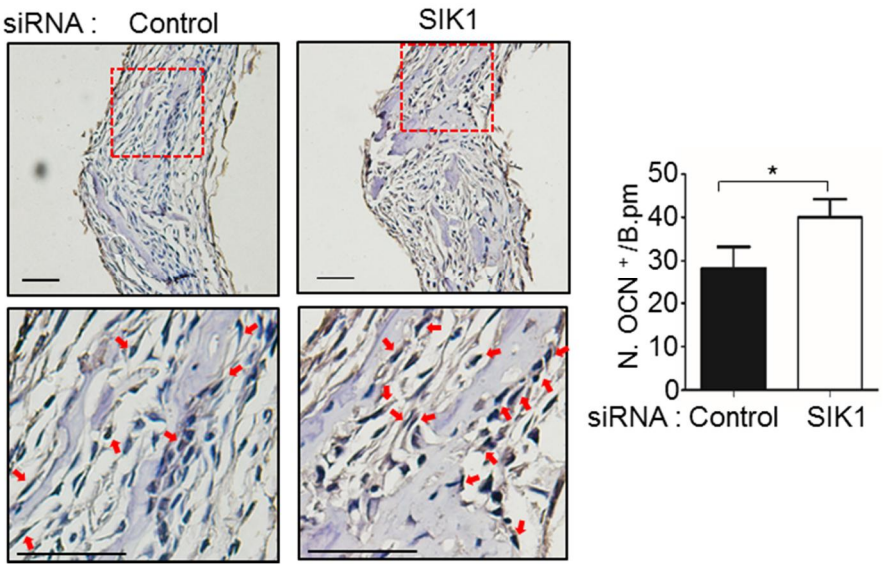

Figure 17. The *ex vivo* downregulation of SIK1 gene increases osteoblast numbers in calvarial bone tissue. Calvariae were transfected with SIK1 siRNA and cultured with osteogenic medium *ex vivo*. Calvarial bones were decalcified and embedded with paraffin. Bone tissue were immunostained with anti-OCN. OCN-positive cells on bone surface around the sagittal suture were

scored. Magnified images of the red boxes in upper panels are shown in bottom panels with arrows indicating OCN-positive cells. Scale bars, 50 μm. *, $p < 0.05$. t-test.

3.4. SIK1 overexpression reduces osteoblast differentiation and matrix mineralization

To assess the effects of SIK1 overexpression, primary preosteoblasts were transfected with a HA-tagged SIK1 expression vector. A successful ectopic overexpression of SIK1 was validated by Western blotting with anti-HA (Figure 18A). ALP staining was much weaker in SIK1 overexpressing cells than in control group cells (Figure 18B). In mineralization assays, SIK1-overexpressing cells showed reduced Alizarin Red staining as compared with the control cells (Figure 19). Consistently, the induction of *Sp7*, *Alp*, and *Col1a1* mRNA by osteogenic medium was significantly attenuated by SIK1 overexpression (Figure 20). As in SIK1 knockdown experiments, the Runx2 protein levels were increased without change of *Runx2* transcription in SIK1 overexpressed group (Figure 21A and 21B). SIK1 overexpression also had negative effects on the osteoblastic differentiation of C2C12 cells in cultures

with BMP2 (Figure 22).

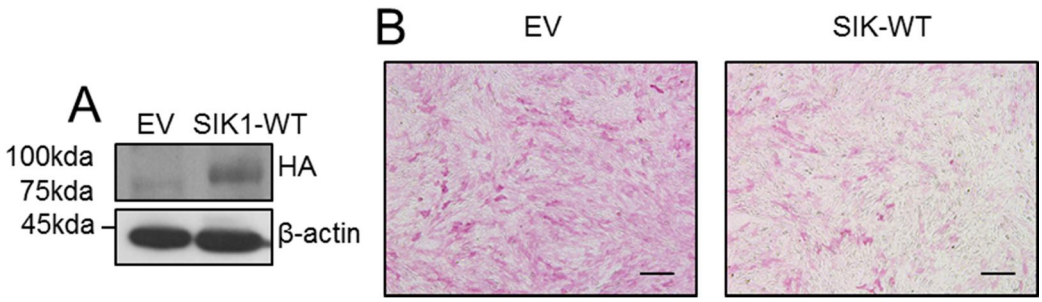

Figure 18. SIK1 overexpression inhibits osteoblast differentiation. (A, B) Primary preosteoblasts were transfected with pcDNA3-SIK1-HA or pcDNA3 (EV). (A) The protein expression levels of SIK1 were analyzed by Western blotting. (B) Transfected cells were cultured in osteogenic medium and stained for ALP activity at day 3. Scale bars, 200 μm.

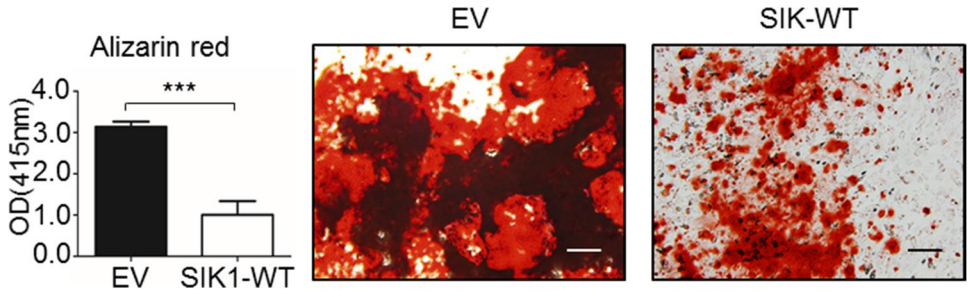

Figure 19. SIK1 overexpression decreases activity of matrix mineralization. Preosteoblasts transfected with SIK1 or EV were cultured with osteogenic medium. Mineralization was evaluated by Alizarin Red staining. ***, $p < 0.001$ versus control. t-test. ***, $p < 0.001$ versus control. t-test. Scale bars, 200 μm.

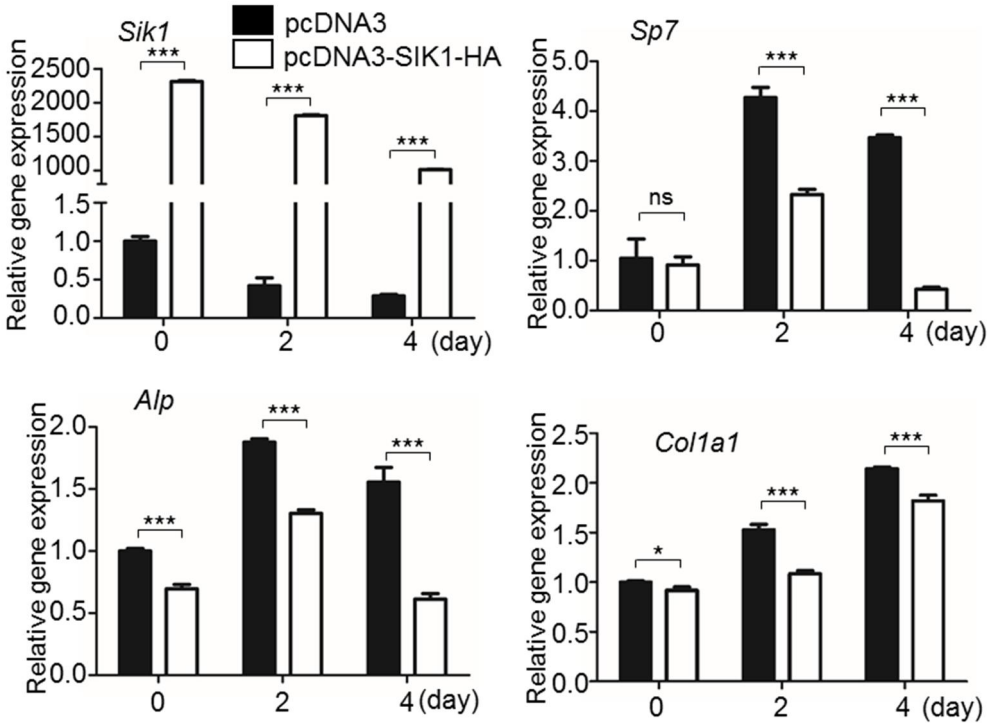

Figure 20. SIK1 overexpression inhibits osteoblastic gene expression. SIK1 overexpressed cells were cultured in osteogenic medium and harvested for real-

time PCR analyses for *Sik1*, *Sp7*, *Alp*, and *Col1a1* mRNA levels. ***, $p < 0.001$.

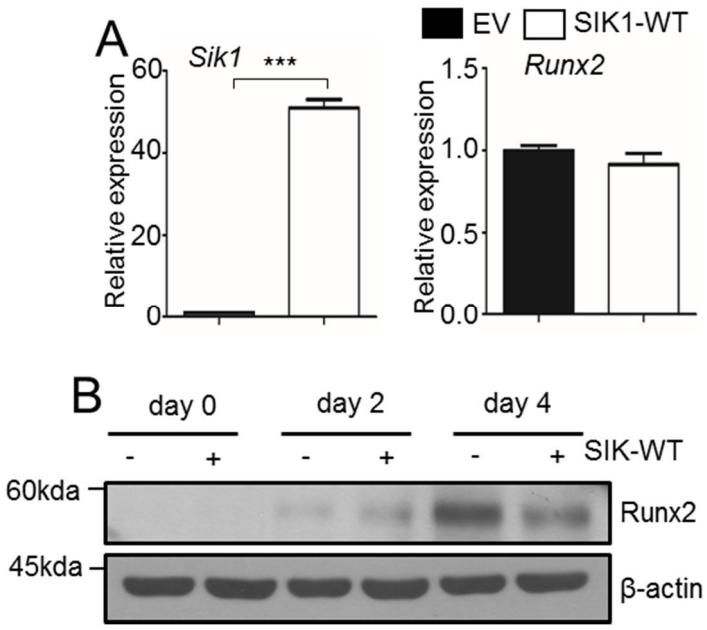

Figure 21. SIK1 overexpression inhibits the expression of Runx2 protein not mRNA. (A, B) Preosteoblasts were transfected with empty vector or SIK1 expression vector and then cultured with osteogenic medium. (A) After 3 days of culture, *Sik1* and *Runx2* mRNA levels were assessed by real-time PCR. (B)

The level of Runx2 protein was detected by Western blotting. ***, $p < 0.001$ verse control.

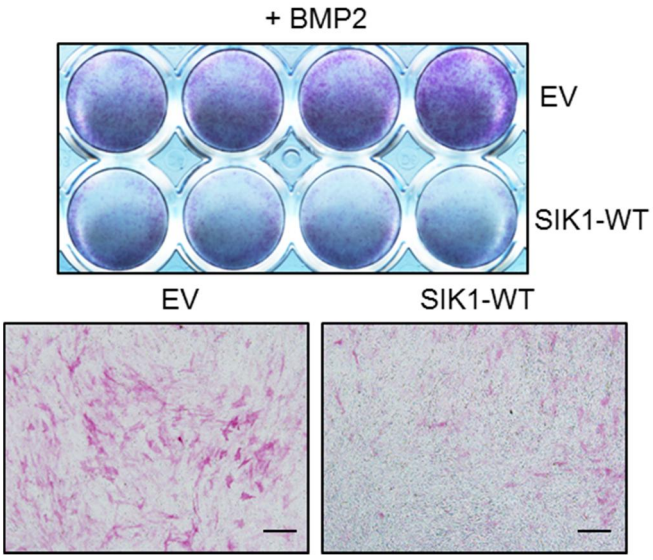

Figure 22. SIK1 overexpression inhibits BMP2-induced osteoblast differentiation of C2C12. C2C12 cells were transfected with control EV or SIK1-WT expression plasmids. Cells were cultured with hBMP2 (150 ng/ml) and subjected to ALP staining. Scale bars, 200 μm.

3.5. SIK1 regulates osteogenesis by affecting preosteoblast proliferation

In osteoblastic differentiation cultures of calvarial preosteoblasts and C2C12 cells, a tendency of a decrease in cell number by SIK1 deficiency was observed (Figure 7B, Figure 11, Figure 13, Figure 18, and Figure 22). In quantitative assays, SIK1 knockdown increased, while SIK1 overexpression decreased, the proliferation of C2C12 cells (Figure 23). To override the effect of different cell number at the start of differentiation culture, equal number of C2C12 cells that had been transfected with siRNA or overexpression plasmid was re-seeded at the initiation of differentiation induction. In these cultures, ALP activity was still higher in SIK1-knockdowned cells and lower in SIK1 overexpressing cells (Figure 24). Similarly, SIK1 WT preosteoblasts showed lower proliferation compared with SIK1 KO cells (Figure 25). Even when the seeding density of WT cells was modulated to have the number of cells similar

to that of KO cells during the culture, ALP activity was significantly lower in WT than in KO cell culture (Figure 26). These data suggest that SIK1 regulates osteogenesis by modulating both the proliferation of precursor cells and the expression of osteoblastic genes.

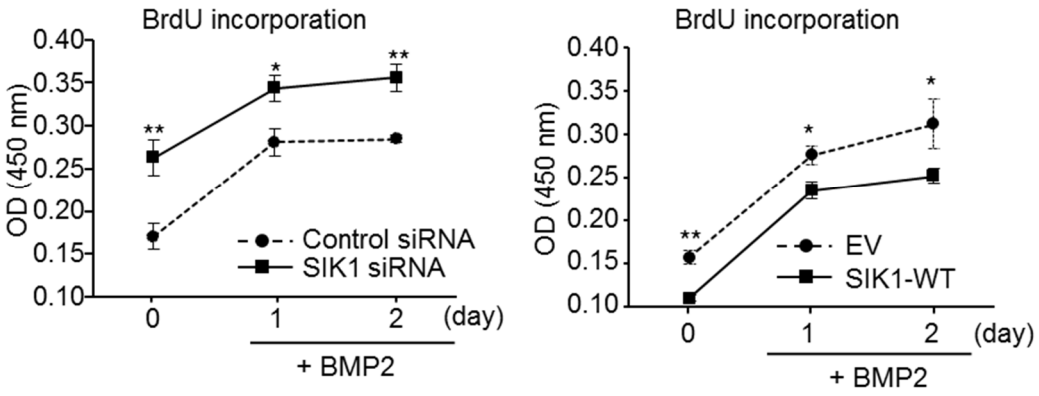

Figure 23. SIK1 affects the proliferation of osteoblast precursors. C2C12 cells were transfected with control or SIK1 siRNA (left), or with control EV or SIK1-WT expression plasmids (right). Cells were cultured with hBMP2 (150 ng/ml) for the indicated days and subjected to the BrdU incorporation assay.

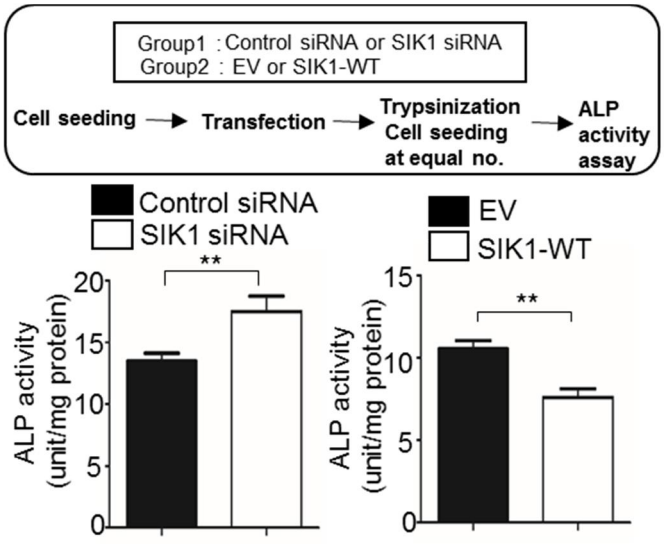

Figure 24. SIK1 regulates osteogenesis by affecting not only preosteoblast proliferation but also osteoblast differentiation. After transfection of C2C12 cells with siRNA or expression plasmids and overnight culture, cells were reseeded at the same density and treated with BMP2 for 2 days. ALP activity

was measured with cell lysates.

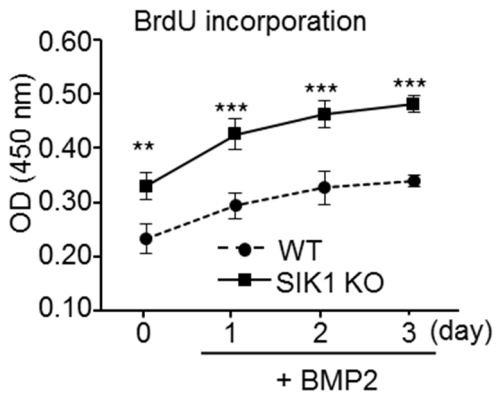

Figure 25. SIK1 KO increases the population of preosteoblast *in vitro*. Calvarial preosteoblasts from WT and SIK1 KO mice were treated with hBMP2 (150 ng/ml) for 3 days and subjected to the BrdU incorporation assay. ***, $p < 0.001$; **, $p < 0.01$. t-test.

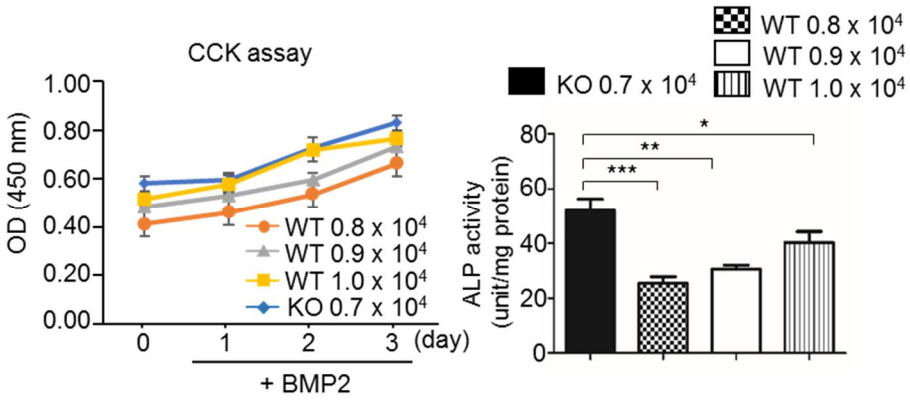

Figure 26. SIK1 KO enhances osteoblast differentiation. Calvarial preosteoblasts from WT and SIK1 KO mice were seeded at the indicated density and treated with BMP2 (150 ng/ml) for 3 days. The CCK assay and ALP activity assay were performed.

3.6. Kinase activity of SIK1 is required for regulation of osteogenesis

SIK1 is a kinase that affects gene expression by phosphorylating transcription regulators. Therefore, it was investigated whether SIK1 modulates osteogenesis by way of its kinase activity. SIK1-T182A plasmid, known as the kinase-dead form of SIK1, was employed (Lizcano, Göransson et al., 2004). Overexpression of SIK1-T182A increased ALP staining, whereas SIK1-WT overexpression decreased ALP staining (Figure 27). Consistently, matrix mineralization activity was reduced by SIK1-WT overexpression and enhanced by SIK1-T182A overexpression (Figure 28). Similar effects of ALP staining in SIK1-WT and SIK1-T182A overexpression were also observed in the context of C2C12 cells (Figure 29). We examined the effect of HG-9-91-01, a pan SIK kinase inhibitor, on osteoblast differentiation. HG-9-91-01 treatment increased ALP staining and ALP activity at concentrations as low as 20 nM in the osteogenic culture of primary preosteoblasts (Figure 30). These data indicate

that the kinase activity of SIK1 is important to its inhibitory role in osteoblast differentiation and matrix mineralization.

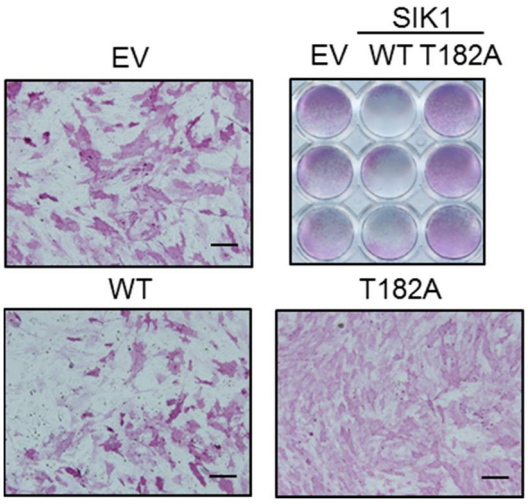

Figure 27. Kinase activity of SIK1 mediates osteoblastic differentiation. Primary preosteoblasts transfected with SIK1-WT, SIK1-T182A, or the control plasmid (EV) were cultured in osteogenic medium for four days. Cells were stained for ALP. Scale bars, 200 μm.

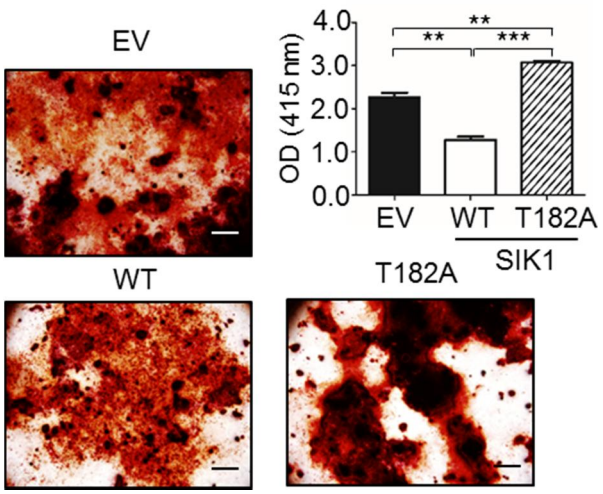

Figure 28. Kinase-inactivation of SIK1 enhances osteoblast mineralization. Primary preosteoblasts transfected with SIK1-WT, SIK1-T182A, or EV were cultured in osteogenic medium for 14 days before Alizarin Red staining. ***, $p < 0.001$; **, $p < 0.01$. t-test. Scale bars, 200 μm.

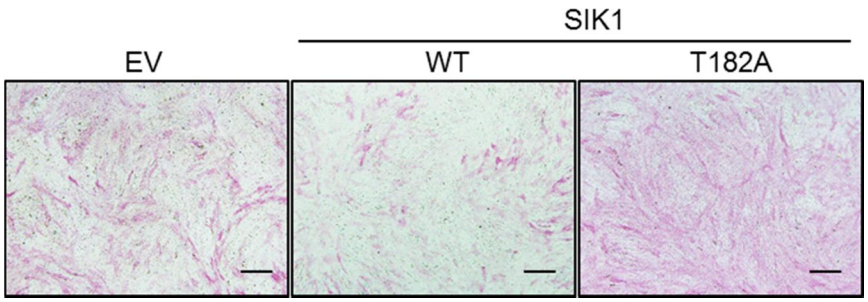

Figure 29. SIK1 catalytic activity regulates osteoblast differentiation of C2C12. C2C12 cells were transfected with pcDNA3-SIK1-WT, pcDNA3-SIK1-T182A, or EV plasmid. Cells were treated with hBMP2 (150 ng/mL) for three days and stained for ALP activity. Scale bars, 200μm.

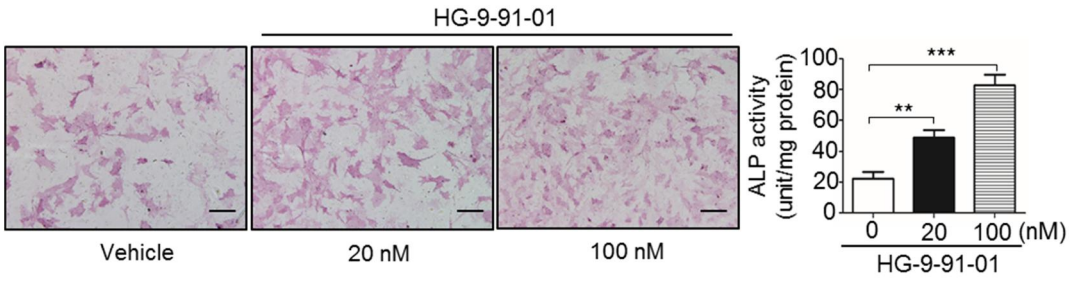

Figure 30. SIKs catalytic inhibition increases osteoblast differentiation in primary preosteoblasts. Primary preosteoblasts were cultured in osteogenic medium containing either vehicle (DMSO) or HG-9-91-01 for three days. Cells were then stained for ALP (left) or subjected to quantitative ALP activity assay (right). Scale bars, 200 μm.

3.7. CRTC1 mediates effect of SIK1 in osteogenesis

It has been reported that SIK1 regulates CREB transcription activity by phosphorylating and thereby suppressing CRTC1 in neurons (Li, Zhang et al., 2009) and that CREB is an important transcription factor for osteogenesis (Siddappa et al., 2008; Kim et al., 2013). Therefore, it was hypothesized that SIK1 might modulate osteogenesis via CRTC and CREB. We first examined the possibility of CRTC1 as a target of SIK1 in osteogenesis regulation. SIK1-WT and SIK1-T182A mutant were overexpressed and CRTC1 phosphorylation at Ser151, the target site of SIKs, was determined in BMP2-treated C2C12 cells. As shown in Figure 31, SIK1-WT greatly increased CRTC1 phosphorylation, whereas T182A suppressed CTRC1 phosphorylation. Phosphorylated CRTCs are sequestered in the cytoplasm (Screaton et al., 2004; Katoh, Takemori et al., 2006; Li, Zhang et al., 2009). Consistently, treatment with the SIK inhibitor HG-9-91-01 increased nuclear and decreased cytoplasmic CRTC1 levels in primary preosteoblasts (Figure 32). To determine whether CRTC1 mediates the function of SIK1 in osteogenesis regulation, we

next examined the effects of CRTC1 downregulation on the enhancement of osteogenesis by SIK1 knockdown. In preosteoblasts cotransfected with SIK1 siRNA and CRTC1 siRNA, mRNA levels of *Sik1* and *Crtc1* were specifically downregulated without interfering with each other (Figure 33). The addition of CRTC1 siRNA blunted the increase in ALP activity by SIK1 knockdown in preosteoblasts (Figure 34). Consistently, the increases in mRNA levels of *Alp*, *Sp7*, *Bglap*, and *Col1a1* by SIK1 siRNA were significantly attenuated by CRTC1 siRNA (Figures 35). These results suggest that SIK1 regulates osteoblast differentiation via CRTC1.

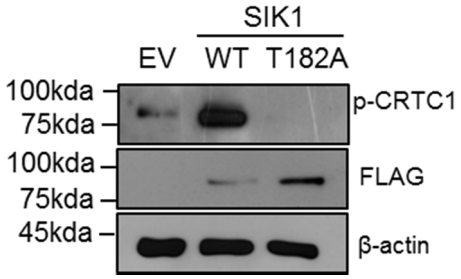

Figure 31. SIK1 mediates phosphorylation of CRTC1 in osteoblast. SIK1-WT-FLAG, SIK1-T182A-FLAG, or the control plasmid (EV) were transfected to C2C12 cells. After stimulation with hBMP2 (500 ng/mL) for 15 minutes, cell lysates were prepared and subjected to Western blotting to assess CRTC1 phosphorylation.

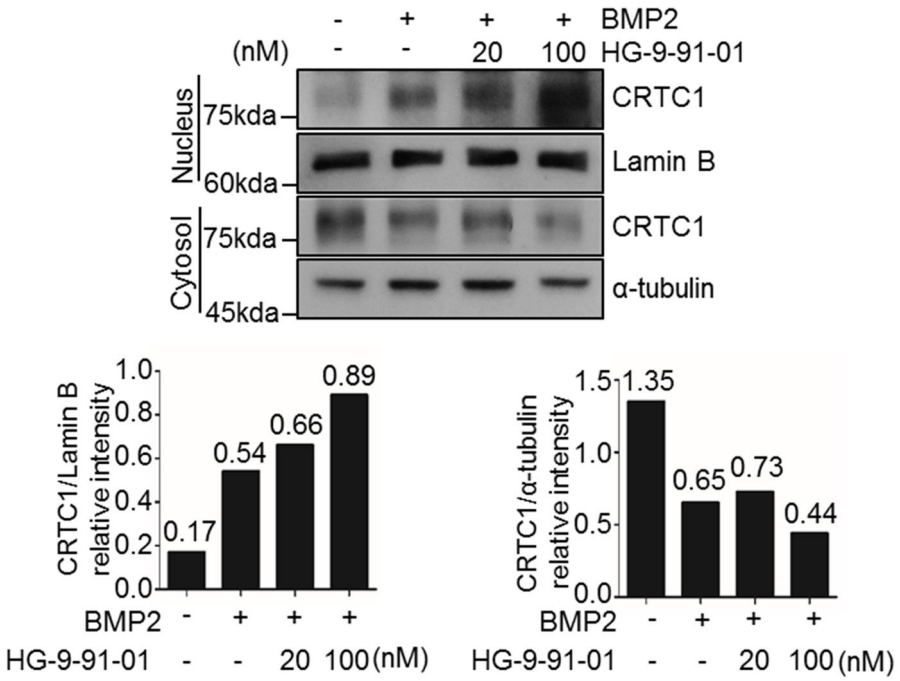

Figure 32. SIK1 regulates the translocation of CRTC1 to nucleus. Primary preosteoblasts were stimulated with hBMP2 in the presence of HG-9-91-01 for

20 minutes. Nuclear and cytoplasmic proteins were analyzed by Western blotting. Nuclear CRTC1 was normalized to Lamin B and cytoplasmic CRTC1 was normalized to alpha-tubulin.

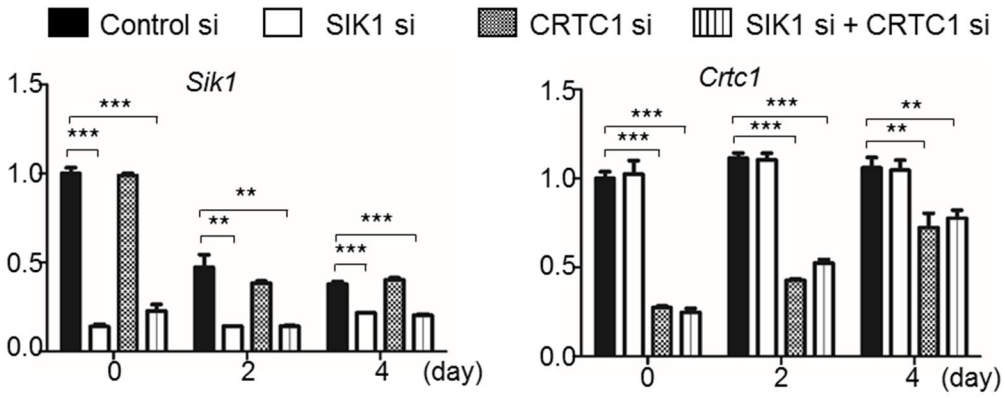

Figure 33. Reduction of SIK1 and CRTC1 gene expression by siRNA was verified in primary preosteoblasts. Primary preosteoblasts were transfected with SIK1 siRNA, CRTC1 siRNA, a combination of SIK1 siRNA and CRTC1 siRNA, or control siRNA. The total amount of siRNA was ensured to be the same in all groups by using additional amounts of control siRNA. Cells were cultured in osteogenic medium for four days and the mRNA levels of SIK1 (A)

and CRTC1 (B) were analyzed by real-time PCR. ***, $p < 0.001$; **, $p < 0.01$ versus control. t-test.

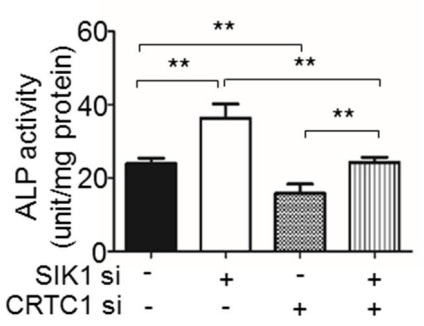

Figure 34. CRTC1 mediates the effect of SIK1 knockdown on ALP activity. Preosteoblasts co-transfected with SIK1 siRNA and CRTC1 siRNA were cultured with osteogenic medium for three days. Cells lystates were subjected to ALP activity assay.

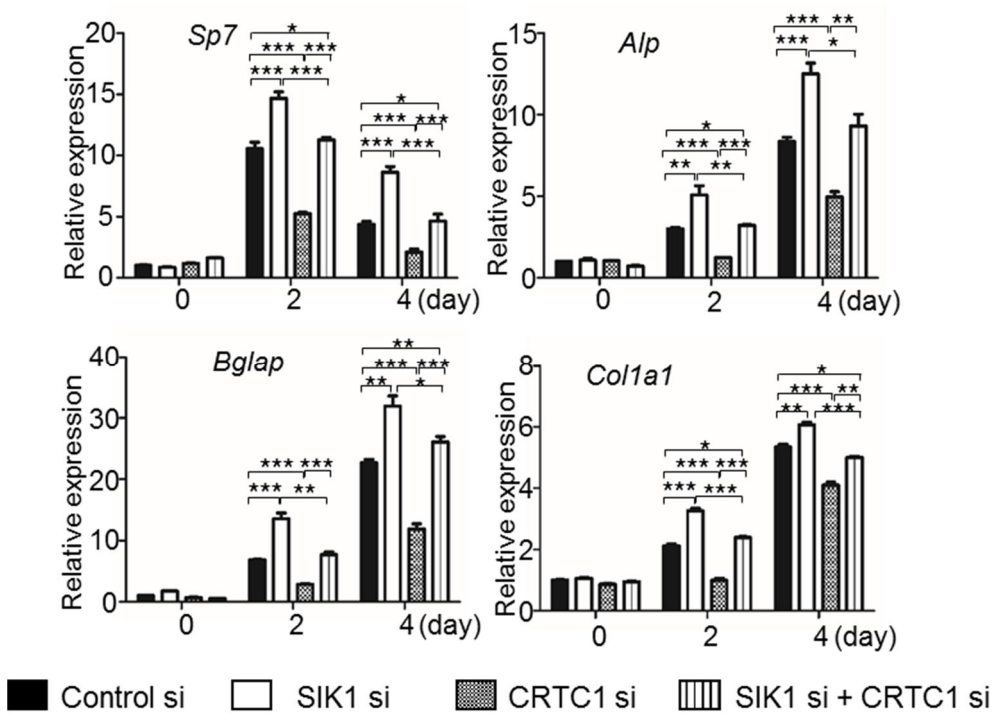

Figure 35. CRTC1 mediates the regulation of osteogenic genes by SIK1. Cells co-expressed with SIK1 and CRTC1 siRNA were cultured with

osteogenic medium. Real-time PCR analyses for *Alp*, *Sp7*, *Bglap*, and *Col1a1* mRNA were performed. ***, $p < 0.001$; **, $p < 0.01$; *, $p < 0.05$.

3.8. SIK1 regulates osteogenesis through a CREB–Id1 axis

As the function of SIK1 in osteogenesis regulation was found to be mediated by the CREB coactivator CRTC1, the effects of SIK1 knockdown in the transcriptional activity of CREB were examined by using a CRE-reporter plasmid. The activity of CRE-luciferase reporter was increased by BMP2 and was further increased by SIK1 knockdown (Figure 36A). On the contrary, SIK1 overexpression suppressed the activity of BMP2-stimulated CRE reporter activity (Figure 36B). CREB can bind the CRE site in the promoter of Id1, an early response gene induced by BMPs (Maeda et al., 2004; Ohta et al., 2008). Therefore, using a luciferase reporter for the Id1 promoter, the potential role of SIK1 in BMP2-dependent Id1 regulation was evaluated. Similar to previous reports (Ogata et al., 1993; Korchynskyi and ten Dijke, 2002), the stimulation of Id1 promoter activity by BMP2 was confirmed (Figure 37). This stimulation was attenuated by the overexpression of SIK1-WT and augmented by the overexpression of SIK1-T182A (Figure 37). Consistently, the BMP2 induction

of Id1 protein expression was potentiated by SIK1 siRNA or SIK1-T182A (Figure 38A) and reduced by the overexpression of SIK1-WT (Figure 38A and B). Furthermore, the induction of both CRE and Id1 promoter reporter activities by SIK1 knockdown was suppressed by the cotransfection of CRTC1 siRNA (Figure 39). The protein expression pattern of Id1 was consistent with the results of reporter assays (Figure 40). These data indicate that SIK1 inhibits osteoblast differentiation by interfering with the CRTC1–CREB–Id1 axis.

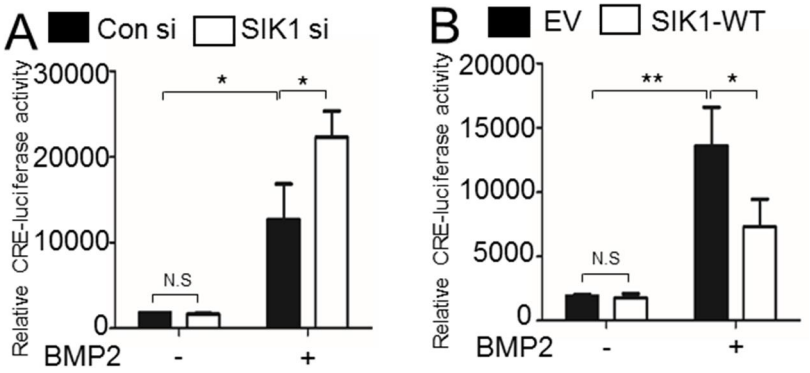

Figure 36. SIK1 regulates BMP2-induced CREB transcriptional activity. A CRE-luciferase reporter plasmid together with the indicated siRNA or pcDNA3 plasmid were transfected to C2C12 cells. Cells were treated with vehicle or hBMP2 (150 ng/mL) for 12 hours. Luciferase assay was performed with cell

lysates. **, $p < 0.01$; *, $p < 0.05$. t-test.

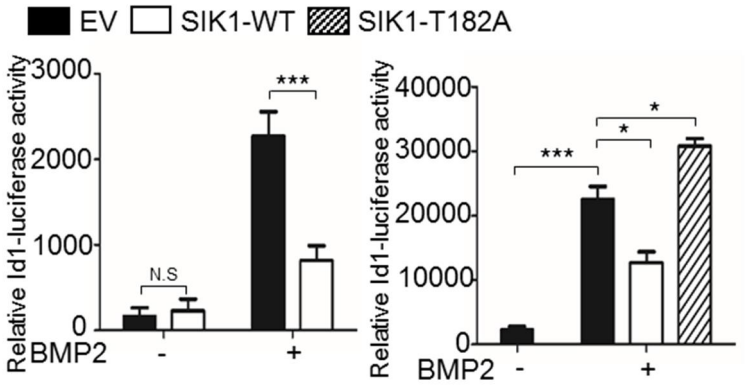

Figure 37. SIK1 regulates BMP2-induced Id1 transcriptional activity. An Id1 reporter together with pcDNA3, SIK1-WT, or SIK1-T182A plasmid were transfected to C2C12 cells. After treating with hBMP2 (150 ng/mL) for 12 hours, cell lysates were subjected to luciferase assay. ***, $p < 0.001$; **, $p <$

0.01; *, $p < 0.05$. t-test.

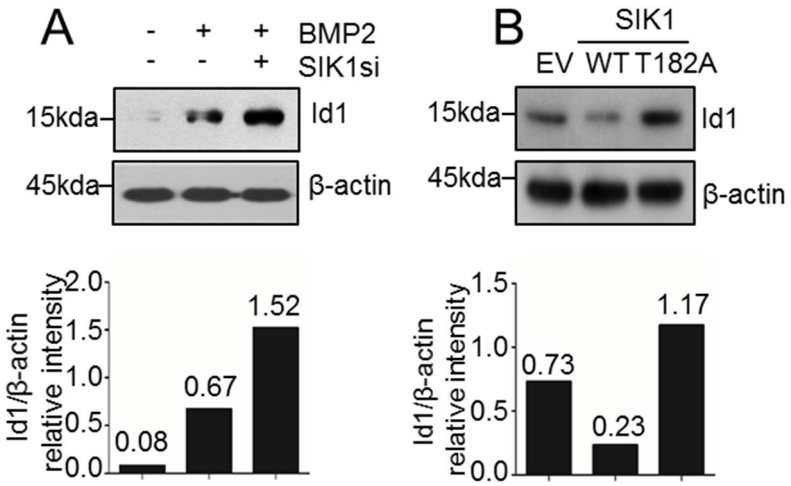

Figure 38. SIK1 regulates the expression of Id1 protein. C2C12 cells transfected with (A) SIK1 siRNA or (B) indicated SIK1 plasmid were treated with hBMP2 (150 ng/mL) for 18 hours. The level of Id1 protein was

determined by Western blotting. Relative Id1 band intensities are presented as histograms.

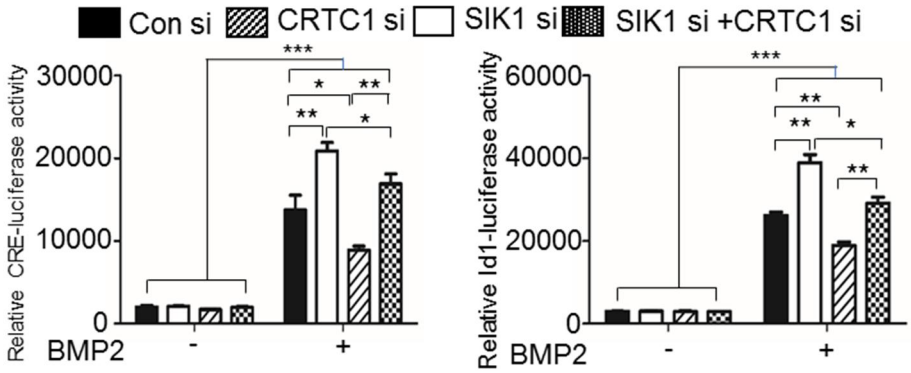

Figure 39. CRTC1 mediates the regulation of the transcriptional activities of CREB and Id1 by SIK1. Primary preosteoblasts co-transfected with SIK1 siRNA and CRTC1 siRNA were stimulated with hBMP2 (150 ng/mL) for 12

hours. CRE and Id1 luciferase assays were performed. ***, $p < 0.001$; **, $p < 0.01$; *, $p < 0.05$.

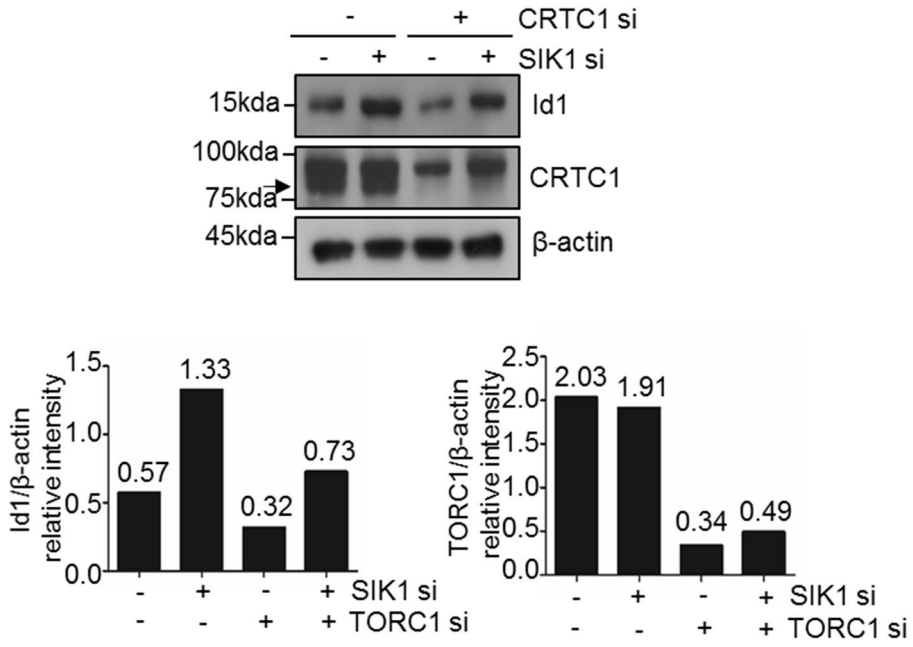

Figure 40. CRTC1 regulates the expression of Id1 protein by SIK1. Primary

preosteoblasts co-transfected with SIK1 siRNA and CRTC1 siRNA were stimulated with hBMP2 (150 ng/mL) for 18 hours. Id1 protein levels were analyzed by Western blotting. The levels of Id1 and CRTC1 were normalized to β-actin. The arrow indicates the CRTC1 band below a nonspecific band.

3.9. SIK1 KO mice display enhanced bone formation

To gain evidence for an *in vivo* relevancy of the *in vitro* and *ex vivo* results of SIK1 knockdown on osteogenesis, the bone phenotype of SIK1 KO mice was evaluated. Gene KO of SIK1 did not affect the SIK2 and SIK3 expression levels (Figure 12). Femurs of 10-week-old female SIK1 KO or littermate WT mice were analyzed by μCT. Three-dimensional images showed trabecular bone mass evidently higher in SIK1 KO than in WT mice (Figure 41A). Quantitative μCT analyses indicated that SIK1 KO bones had significantly higher trabecular bone volume/total volume (BV/TV), thickness (Tb.Th), and trabecular number (Tb.N), and lower trabecular separation (Tb.sp), respectively, as compared with WT bones. Cortical BV/TV (Ct.BV/TV) and cortical thickness (Ct.Th) were also significantly higher in KO than in WT femurs (Figure 41B). In male mice, KO femurs showed significantly higher Tb.Th and Tb.N values with a tendency for increased Tb.BV/TV and Ct.BV/TV

values as compared with WT femurs (Figure 42).

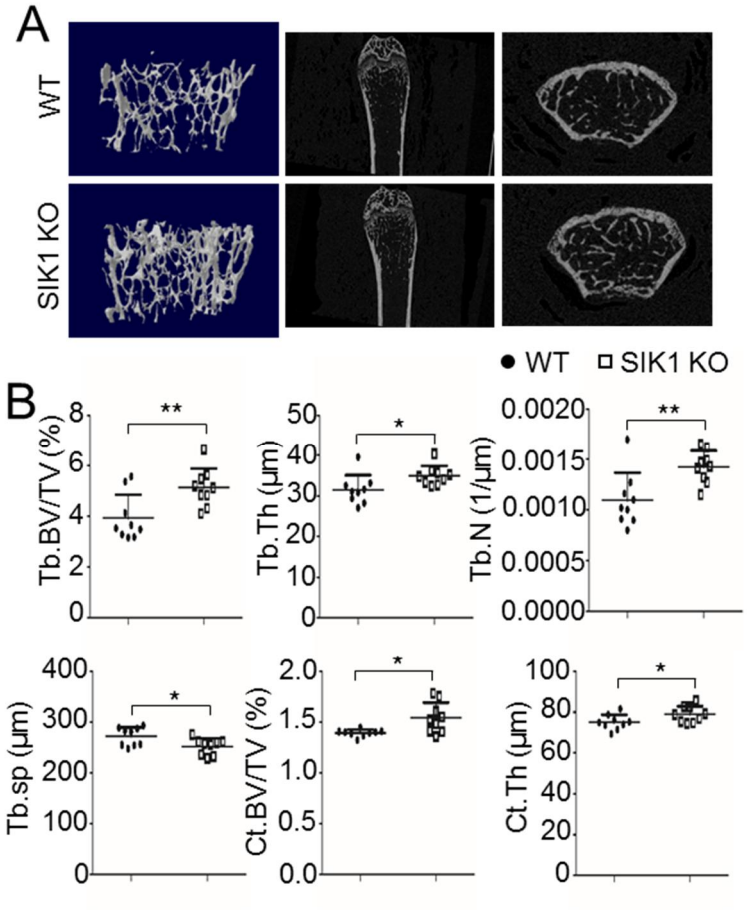

Figure 41. Female mice of SIK1 KO display enhanced bone formation. (A,

B) Femurs of 10-week-old SIK1 KO and littermate WT female mice were analyzed by μCT (n = 9 per group). (A) Three-dimensional images of trabecular bone reconstructed with Skyscan CTvol software (left), and two-dimensional sagittal (middle) and transaxial (right) images produced with the DataViewer software are shown. (B) Trabecular and cortical bone parameters obtained by μCT analyses are presented. Trabecular bone parameters; trabecular bone volume/total volume (Tb.BV/TV), trabecular thickness (Tb.Th), trabecular number (Tb.N), and separation (Tb.sp), and cortical bone parameters; cortical BV/TV (Ct.BV/TV) and cortical thickness (Ct.Th).

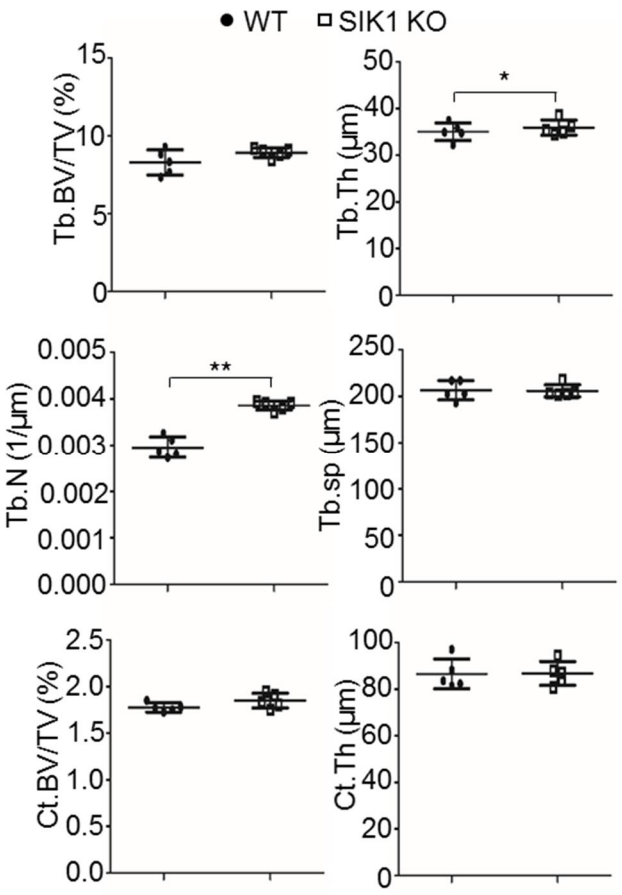

Figure 42. Male mice of SIK1 KO display a tendency for increased bone formation. Femurs of 10-week-old SIK1 KO and littermate WT male mice were analyzed by μCT (n = 5 per group). Trabecular bone volume (Tb.BV/TV), thickness (Tb.Th), number (Tb.N), separation (Tb.sp), and cortical bone volume (Ct.BV/TV) and thickness (Ct.Th) indices were presented. **, $p < 0.01$, *, $p < 0.05$ versus WT.

3.10. SIK1 deficiency enhances activity of osteoblast, but not osteoclast

Next, it was investigated whether the increased bone mass of SIK1 KO was due to the increase of bone anabolic effect by osteoblast or the decrease of bone catabolic effect by osteoclast. To this end, histomorphometric analyses were performed. Decalcified femur sections were subjected either to Goldner's trichrome staining to obtain osteoblast-related parameters or to TRAP staining to gain osteoclast-associated parameters. Osteoblast number per bone perimeter (N.OB/B.Pm) and osteoblast surface per bone surface (OB.S/BS) were significantly increased by SIK1 deficiency (Figure 43). In contrast, osteoclast number per bone perimeter (N.OC/B.Pm) and osteoclast surface per bone surface (OC.S/BS) were not different between WT and KO mice (Figure 44). There was also no difference regarding RANKL/OPG ratio in the sera of WT and KO mice (Figure 45). Osteoclastogenic cultures of BMMs from SIK1 KO and WT mice showed no difference between the two groups with respect to the number of osteoclasts identified by TRAP staining (Figure 46A). In addition, there was no difference in the expression levels of osteoclast marker genes *Nfatc1* and *Acp5* (Figure 46B). Similarly, SIK1 knockdown cells by siRNA did affect osteoclast differentiation (Figure 47). Furthermore, calcein double

labeling experiments revealed a higher bone anabolic activity in KO mice, with significant increases in mineralized surface per bone surface (MS/BS), mineral apposition rate (MAR), and bone formation rate per bone surface (BFR/BS) (Figure 48). Based on these *in vivo* and *in vitro* analyses, it is reasonable to conclude that the increased bone mass in SIK1 KO mice is mainly due to the effect of SIK1 deficiency in osteoblast-lineage cells, not to an indirect systemic attribution or an inhibition of osteoclast activity.

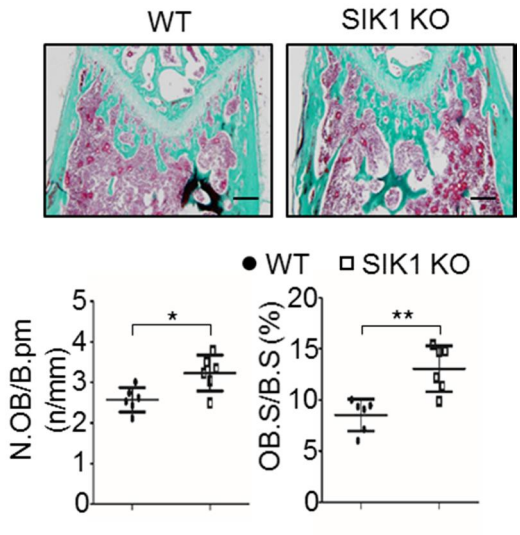

Figure 43. Femoral bone of SIK1 KO mice increases osteoblastic parameters in histomorphometric analyses. Decalcified femur of WT or SIK1 KO mice sections were stained with Goldner's trichrome. Stained sections were analyzed with Osteomeasure software to obtain N.OB/B.pm, OB.S/B.S. **, $p < 0.01$; *, $p < 0.05$. Scale bars, 200 μm.

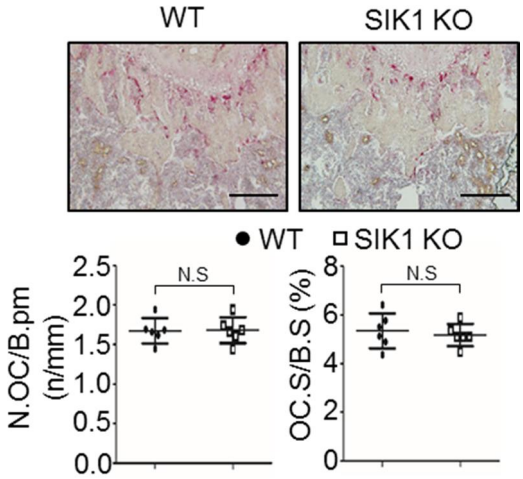

Figure 44. Histomorphometric analyses of femoral bone display no difference in osteoclastic parameters between WT and SIK1 KO mice. Decalcified sections of WT or SIK1 KO femoral bones were stained for TRAP activity. From the stained sections, the indices of osteoclast number per bone perimeter (N.OC/B.Pm), and osteoclast surface per bone surface (OC.S/BS) were obtained. Scale bars, 200 μm.

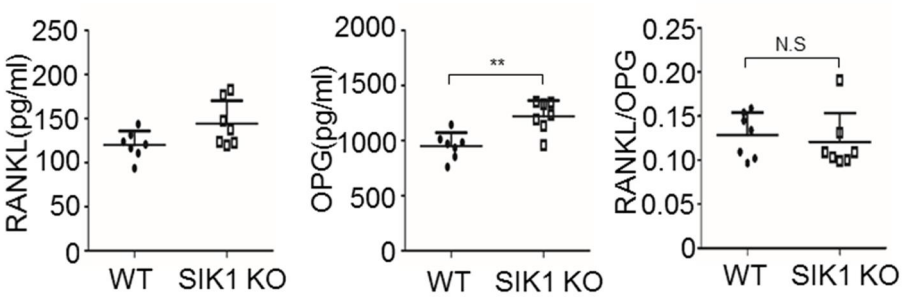

Figure 45. No difference in RANKL/OPG ratio in the serum of WT and KO mice. Serum RANKL and OPG levels of WT or SIK1 mice were assessed with ELISA kits. **, $p < 0.01$. N.S, not significant.

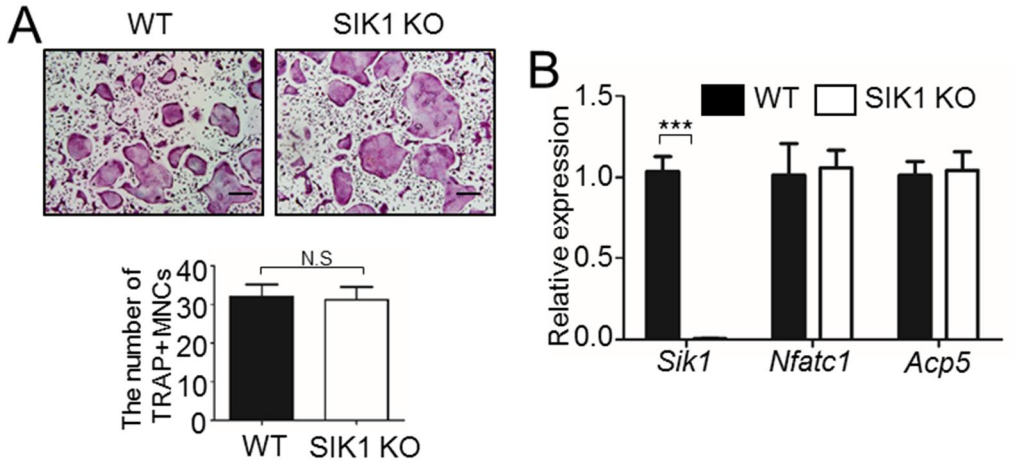

Figure 46. SIK1 KO does not affect osteoclast differentiation. (A) BMMs from WT or SIK1 KO mice were cultured with M-CSF (30 ng/mL) and RANKL (150 ng/mL). After four days, cells were stained for TRAP and TRAP-positive multinuclear cells were counted. Scale bars, 200 μm. (B) BMMs from WT or SIK1 KO mice were cultured with M-CSF (30 ng/mL) and RANKL (150 ng/mL). The mRNA levels of *Sik1*, *Nfatc1*, and *Acp5* were analyzed by real-time PCR. N.S, not significant. ***, $p < 0.001$.

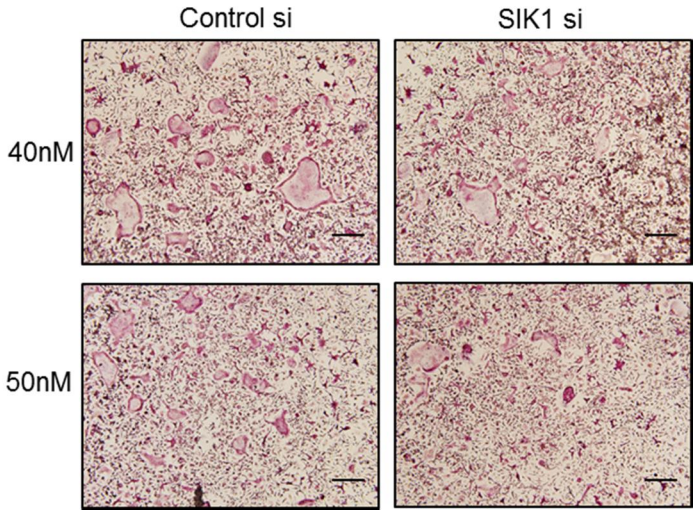

Figure 47. SIK1 knockdown does not affect osteoclast differentiation. BMMs transfected with SIK1 siRNA or control siRNA (40 nM or 50 nM) were cultured with medium containing M-CSF (30 ng/mL) and RANKL (150 ng/mL). After four days, cells were stained for TRAP and TRAP-positive multinuclear cells were counted. Scale bars, 200 μm.

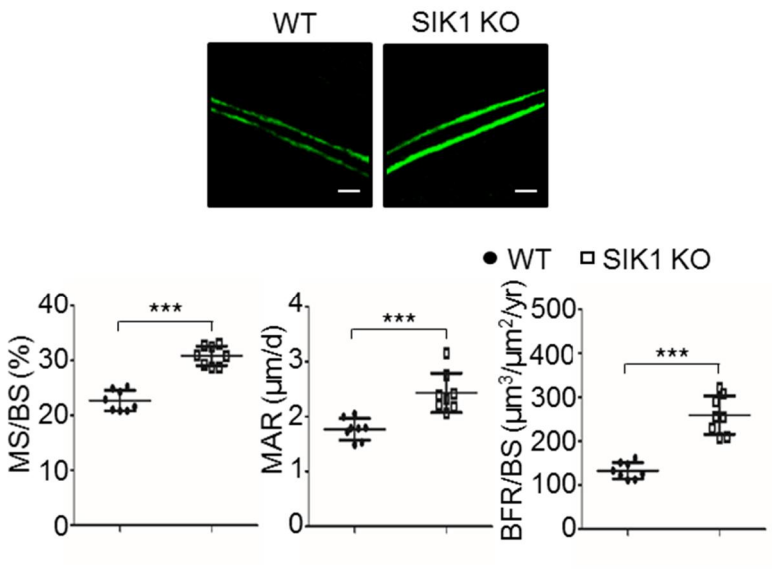

Figure 48. SIK1 KO increases bone formation activity. WT and SIK1 KO mice were injected with calcein as described in Materials and Methods. Femurs without decalcification were embedded in resin. Representative fluorescence images of sectioned slices are shown. Mineralized surface per bone surface (MS/BS), mineral apposition rate (MAR), and bone formation rate per bone surface (BFR/BS) parameters were analyzed with the Osteomeasure software. ***, $p < 0.001$. Scale bars, 20 μm

3.11. SIK1 is selectively downregulated during osteogenesis via a PKA-dependent mechanism

As SIK1 activity negatively regulated bone formation in response to osteogenic stimuli (combination with β-GP and AA, and BMP2), it was also examined whether expression of SIK1 change during BMP2-induced osteogenesis. During osteogenesis, BMP2 treatment decreased the expression of SIK1 protein as well as mRNA (Figures 49A and 49B). Intriguingly, the BMP2-induced downregulation of SIK1 was attenuated by H89, a PKA inhibitor (Figure 49A and 49B). In line with these observations, the PKA activator forskolin enhanced BMP2-induced osteoblast differentiation, while SIK1 knockdown further potentiated the effect of forskolin (Figures 50A and 50B). Forskolin-dependent CRE and Id1 promoter activities were also attenuated by the overexpression of SIK1-WT, but not by that of SIK1-T182A (Figure 51). In addition, forskolin augmented the BMP2 upregulation of Id1 protein level, which was further increased by SIK1 siRNA (Figure 52). These results suggest that the PKA-mediated downregulation of SIK1 is essential for osteogenic differentiation, as SIK1 inhibits the CREB activity involved in the transcription of multiple osteogenic genes.

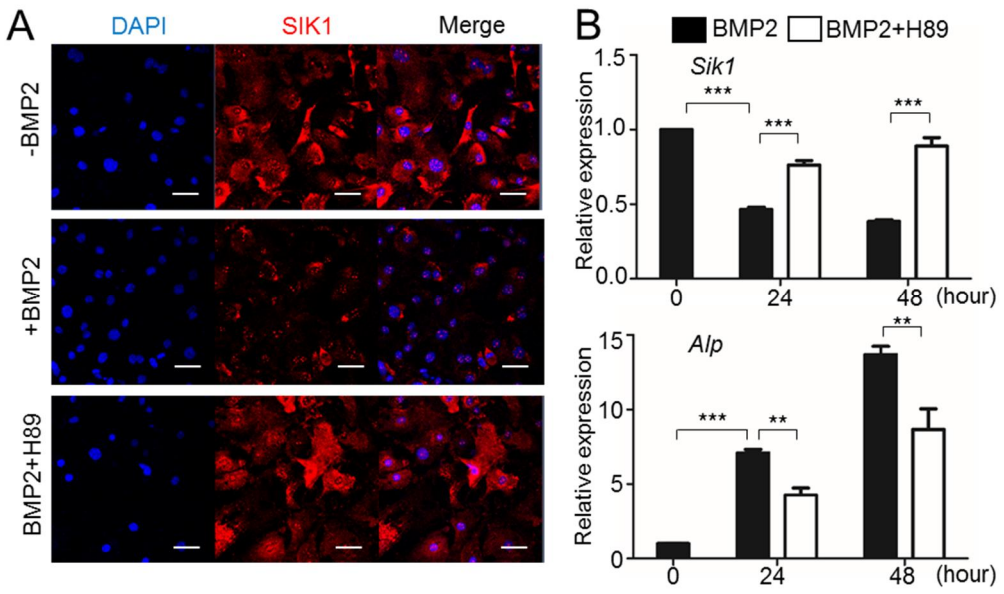

Figure 49. SIK1 is downregulated during BMP2-induced osteogenesis via a PKA-dependent mechanism. (A) Primary preosteoblasts were treated with BMP2 (150 ng/mL) for two days in the absence or presence of H89 (10 μM). The protein expression of SIK1 was analyzed by confocal microscopy (Red: SIK1; Blue: DAPI). (B) Primary preosteoblasts were treated with BMP2 (150 ng/mL) in the absence or presence of H89 (10 μM). The *Sik1* and *ALP* mRNA levels were analyzed by real-time PCR. ***, $p < 0.001$; **, $p < 0.01$, *, $p < 0.05$. Scale bars, 50 μm.

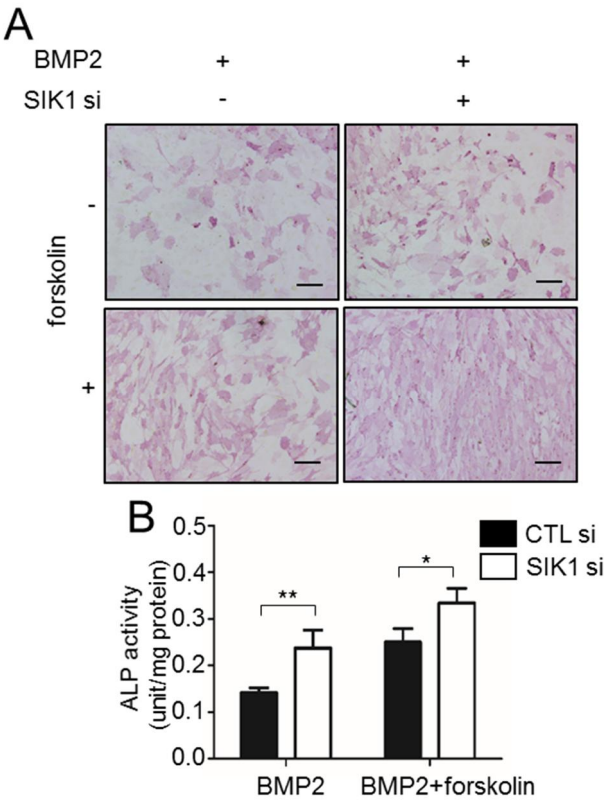

Figure 50. PKA activation increases the ALP induction by BMP2. Primary preosteoblasts transfected with control or SIK1 siRNA were treated with BMP2 (150 ng/mL) for three days in the absence or presence of forskolin (1 μM). Cells were stained for ALP (A) or cell lysates were subjected to ALP activity assay (B). Scale bars, 200 μm.

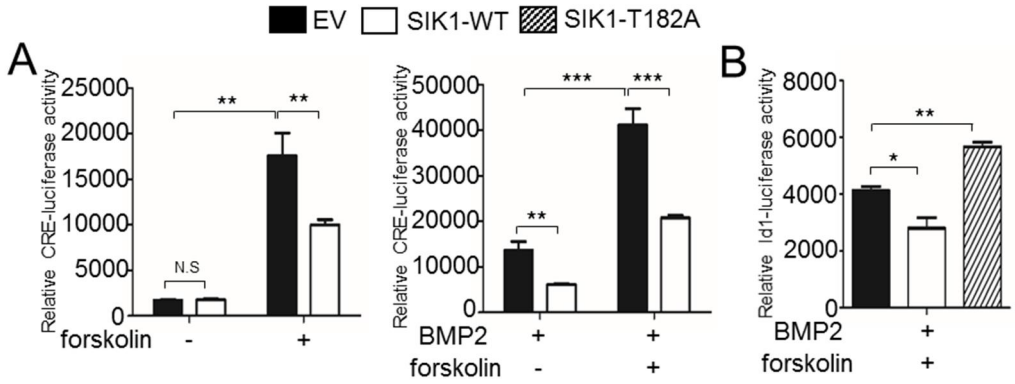

Figure 51. SIK1 suppressed forskolin-induced CRE and Id1 promoter activities. C2C12 cells were transfected with either CRE (A) or Id1 promoter (B) luciferase reporter plasmid together with pcDNA3-SIK1-WT, pcDNA3-SIK1-T182A, or pcDNA3. Cells were stimulated with forskolin (10 mM) alone or together with hBMP2 (150 ng/mL). Cell lysates were prepared and luciferase assays were performed. ***, $p < 0.001$; **, $p < 0.01$; *, $p < 0.05$ versus control. t-test.

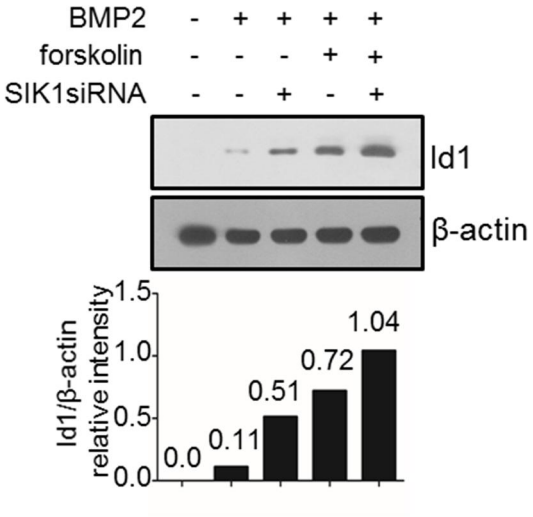

Figure 52. SIK1 mediates the BMP2-induction of Id1 protein via a PKA signaling pathway. C2C12 cells were transfected with SIK1 siRNA and stimulated with hBMP2 (150 ng/mL) in the absence or presence of forskolin (10 μM) for 18 hours. Id1 protein expression was analyzed by Western blotting, and the level of Id1 was normalized to that of β-actin.

4. DISCUSSION

This study demonstrated that SIK1 plays an important role in bone metabolism by regulating osteogenesis *in vitro* and *in vivo*. The *in vitro* experiments also revealed that the CRTC1–CREB–Id1 axis is a key element in the inhibitory function of SIK1 in osteoblast differentiation. In addition, we found that osteogenic factors like BMP2 decreased SIK1 expression levels via a mechanism dependent on PKA to null the antiosteogenic effects of SIK1 (Figure 53). Based on these findings, it is proposed that the suppression of SIK1 activity and subsequent activation of the CRTC1–CREB pathway is a crucial event in bone anabolism.

Other members of the SIK family have recently been reported to be involved in skeletal physiology. These include SIK2, which was shown to mediate PTH responses in osteocytes (Wein, Liang et al., 2016). In this study, PTH induced the repression of *Sost*, a gene encoding the Wnt inhibitor sclerostin, by stimulating the inactivation of phosphorylation of SIK2 in Ocy454 osteocytic cells. Lowered SIK2 activity results in the underphosphorylation of class IIa HDACs (HDAC4 and HDAC5), causing dissociation from its cytoplasmic retainer 14-3-3 and subsequent translocation to the nucleus for repression of Mef2c involved in *Sost* transcription (Wein, Liang et al., 2016). Consistent with the well-recognized bone anabolic effects of

intermittent administration of PTH, once-daily treatment with pan-SIK inhibitors increased bone formation (Wein, Liang et al., 2016). Thus, the regulation of SIK2 in osteocytes may explain the bone-forming action of PTH. Whether SIK1 could also play a role in the osteocyte response to PTH is not clear. However, the findings of that PTH- and SIK-inhibitor-induced *Sost* gene suppression did not occur in SIK2-knockout and SIK2/3 knockdown osteocytes, respectively (Wein, Liang et al., 2016), indicate no significant part played by SIK1 in osteocytes and instead point to the specific roles of each SIK family member in the control of osteoblast-lineage cells in responding to different signals. Nevertheless, both the role of SIK2 in osteocytes and our results showing the role of SIK1 in osteoblasts support the clinical value of SIK inhibitors as bone anabolic agents.

PKA is one of the major signaling molecules of which activation leads to the stimulation of CREB, a transcription factor crucial for bone formation (Siddappa, Martens et al., 2008; Zhao et al., 2009). In response to signals that elevate cAMP levels, activated PKA can directly phosphorylate CREB to enhance its transcription activity (Gonzalez and Montminy, 1989; Lin et al., 1998). Recent findings add another layer of CREB stimulation by PKA, achieved through SIKs (Katoh, Takemori et al., 2006; Sonntag, Vaughan et al.,

2018). In this mechanism, the PKA-dependent phosphorylation of SIKs inhibits their activity in phosphorylating CRTCs, unleashing CRTCs from cytoplasmic retention and facilitating nuclear translocation for CREB binding (Sonntag, Vaughan et al., 2018). This PKA inhibition of the catalytic activity of SIKs may be reinforced by a regulation of the expression levels of SIKs. Indeed, we observed a decrease in SIK1 levels via treatment with forskolin, a PKA activator (data not shown), or under osteogenic medium (Figure 48A). In addition, H89, a PKA inhibitor, blocked the BMP2-dependent reduction of SIK1 levels (Figure 48). Therefore, it appears that the suppression of SIK1 is a requisite in driving osteogenic differentiation, which is ensured by the dual actions of PKA in reducing SIK1 expression level as well as in inhibiting SIK1 catalytic activity (Figure 49B). Interestingly, SIK1 abundance was suggested to be critical for myogenesis and SIK1 mRNA and protein levels were shown to increase during myoblast differentiation (Stewart, Akhmedov et al., 2013). Thus, these results clearly point to contrasting directions in the regulation of expression level of SIK1 during osteogenesis and myogenesis. Whether this distinctive expression pattern of SIK1 is a key element in the fate determination of common mesenchymal progenitor cells of osteoblasts and myoblasts is an intriguing question to be explored in further work.

A recent report has suggested that SIK activity is involved in RANKL-induced osteoclastogenesis (Lombardi et al., 2017). In the study, HG-9-91-01 suppressed osteoclast differentiation from RAW264.7 and BMMs and induced the nuclear translocation of CRTC3 and HDAC5. Either SIK2- or SIK3-silencing by a CRISPR/Cas9 system in RAW264.7 reduced osteoclastogenesis, suggesting that SIK2 and SIK3 may play nonredundant roles, with the lack of SIK2 not being compensated for by the presence of SIK3 and vice versa. Although whether SIK1 was also involved in osteoclastogenesis could not be addressed in the report, Figure 47 indicated no effects of SIK1 knockdown in BMMs on osteoclastic differentiation. There were also no differences in the osteoclast number between WT and SIK1 KO bones and in the RANKL/OPG ratio between WT and KO mice sera (Figures 44 and 45). In this study, SIK1 was distinct from the other isoforms SIK2 and SIK3 in regulating osteoblast differentiation (Figure 7). Besides, Figure 6 showed a decreasing pattern of SIK1 levels unlike the expression of SIK2 and SIK3 in the early time point of osteogenic culture. Although the answer to whether SIK1 is a dominant player in osteoblast regulation while SIK2/3 are more important in osteoclast regulation remains elusive, the demonstration of a predominant role of SIK2 in PTH responses in osteocytes (Wein, Liang et al., 2016) suggests a certain level of specificity in the actions of each member of SIKs. However, these data

showing the control of osteoblast differentiation by SIK1, the study on SIK2 function for PTH responses in osteocytes (Wein, Liang et al., 2016), and the demonstration of SIK2/3 involvement in osteoclastogenesis (Lombardi, Gilliéron et al., 2017) all indicate that SIK inhibition is beneficial for conditions requiring bone mass increases, such as osteoporosis.

SIK1 has different characteristics from the other isoforms SIK2 and SIK3, although SIK family kinases are capable of similarly regulating downstream targets. SIK1 expression is mediated by various stimuli including high salt diet, adrenocorticotropin hormone, cell depolarization, glucagon, and circadian rhythm. In contrast, SIK2 and SIK3 are constitutively expressed in tissues where they are expressed and located on human chromosome 11 (Wein, Foretz et al., 2018). In the previous studies, SIK1 was reported to be important for regulation of myogenesis (Stewart, Akhmedov et al., 2013), and mice deficient for *Sik1* gene showed the increase of insulin sensitivity and glucose consumption in skeletal muscle under a condition of over-nutrition (Nixon et al., 2016). On the other hand, SIK2 and SIK3 was reported be downregulated in adipose tissue of obese or insulin-resistance humans (Sall et al., 2017), and general SIK2 knockout mice revealed the increased white adipocyte, insulin resistance, hyperglycemia, and hypertriglyceridemia (Park et al., 2014). Besides,

SIK1 is expressed lower in tumors than in normal tissues whereas SIK2 and SIK3 are overexpressed in multiple tumors (Du et al., 2016). These reports and the present results suggest differences in the effects of downstream molecules regulated by each SIK isoform or the specific responses of these kinases to various stimuli.

This report showed that the major target of SIK1 in regulating osteogenesis is CRTC1. CRTCs enhance CREB transcription activity by binding to the basic leucine zipper domain of CREB in the nucleus (Conkright et al., 2003; Screaton, Conkright et al., 2004).CRTCs in phosphorylated states are sequestered in the cytoplasm by 14-3-3 binding and thus dephosphorylation is required for the nuclear translocation of CRTCs (Conkright, Canettieri et al., 2003; Katoh, Takemori et al., 2006; Li, Zhang et al., 2009). Our results revealed that the reduction in SIK1 activity during osteoblast differentiation led to a decrease in CRTC1 phosphorylation and an increase in nuclear CRTC1 levels. More importantly, CRTC1 knockdown almost completely blocked the increasing effects of SIK1 knockdown on osteoblast differentiation (Figure 4), suggesting CRTC1, among three CRTCs, to be the major player in the control of osteogenesis. Enhanced CREB activity may be linked to Id gene expression as a CREB binding site is present in the Id1 gene promoter (Lopez-Rovira et al.,

2002) and CREB-stimulators like dibutyryl cAMP and forskolin increased Id transcription (Scobey et al., 2004; Doorn et al., 2012; Zhang, Li et al., 2015). In addition, BMP2 increases Id levels in osteoblast-lineage cells and myoblasts (C2C12) (Ogata, Wozney et al., 1993; Katagiri et al., 1994; Peng et al., 2004) and Ids were shown to have positive roles for bone formation in mice (Maeda, Tsuji et al., 2004). In this study, BMP2-induction of Id1 was regulated by the SIK1–CRTC1 pathway and SIK KO cells had a higher level of Id1 expression versus WT cells. Therefore, the CRTC1–CRE–Id1 pathway appears to be primarily responsible for the control of osteogenesis by SIK1.

Ids function as negative regulators of bHLH-containing transcriptions factors by direct binding and subsequent inhibition of DNA binding of bHLH factors (Benezra et al., 1990; Miyazono and Miyazawa, 2002). Alternatively, Id1 was shown to induce the degradation of Twist1, a bHLH factor that suppresses osteogenic genes, to increase BMP signaling (Hayashi et al., 2007). Liberation from the Twist-mediated inhibition of Runx2 activity was reported to be critical in the initiation of osteoblast differentiation during embryogenesis (Bialek et al., 2004). As Ids counteract Twists, induction of Id1 may also be essential to the maintenance of bone homeostasis by supporting osteogenesis during bone remodeling in adults. In this study, we for the first time revealed a

link between SIK1 activity regulation and BMP2-induction of Id1 for osteoblast differentiation.

In conclusion, these results demonstrate that the suppression of SIK1 activity is a critical event in the initiation and progression of osteogenesis to stimulate precursor proliferation and to induce expression of osteoblastic genes. We also showed that, to achieve SIK1 inhibition, BMP2 reduces SIK1 gene expression and also catalytic activity, both in a PKA-dependent manner. The reduction in SIK1 activity leads to CRTC1–CREB activation, which turns on the osteogenesis program by stimulating the transcription of Id1 and other osteogenic genes. Therefore, SIK1 may be a promising target for the development of novel bone anabolic therapeutics.

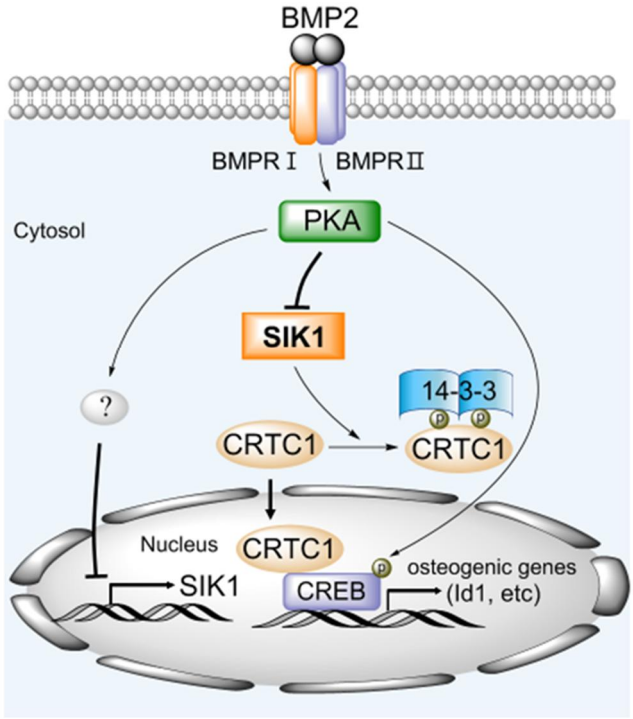

Figure 53. The role of SIK1 in osteoblast differentiation. In the absence of BMP2 signaling, SIK1 phosphorylates CRTC1 and thereby inhibits its nuclear translocation, leading to a suppression of CREB target genes. In response to BMP2, SIK1 level is downregulated and SIK1 activity is inhibited by PKA-dependent mechanisms. Under this SIK1-repressed condition, dephosphorylated CRTC1 translocates into the nucleus and stimulates CREB activity for induction of osteogenic genes including Id1.

5. REFERENCES

Augustine, M. and Horwitz, M.J. (2013) Parathyroid hormone and parathyroid hormone-related protein analogs as therapies for osteoporosis. *Curr Osteoporos Rep* 11, 400-406.

Benezra, R., Davis, R.L., Lockshon, D., Turner, D.L. and Weintraub, H. (1990) The protein Id: A negative regulator of helix-loop-helix DNA binding proteins. *Cell* 61, 49-59.

Berdeaux, R., Goebel, N., Banaszynski, L., Takemori, H., Wandless, T., Shelton, G.D. and Montminy, M. (2007) SIK1 is a class II HDAC kinase that promotes survival of skeletal myocytes. *Nat Med* 13, 597.

Bialek, P., Kern, B., Yang, X., Schrock, M., Sosic, D., Hong, N., Wu, H., Yu, K., Ornitz, D.M., Olson, E.N., et al. (2004) A twist code determines the onset of osteoblast differentiation. *Developmental Cell* 6, 423-435.

Boyle, W.J., Simonet, W.S. and Lacey, D.L. (2003) Osteoclast differentiation and activation. *Nature* 423, 337-342.

Chang, E.J., Ha, J., Oerlemans, F., Lee, Y.J., Lee, S.W., Ryu, J., Kim, H.J., Lee, Y., Kim, H.M., Choi, J.Y., et al. (2008) Brain-type creatine kinase has a crucial role in osteoclast-mediated bone resorption. *Nat Med* 14, 966-972.

Chen, J. and Long, F. (2015) mTORC1 signaling promotes osteoblast differentiation from preosteoblasts. *PLOS ONE* 10, e0130627.

Chen, J.S. and Sambrook, P.N. (2011) Antiresorptive therapies for osteoporosis: a clinical overview. *Nat Rev Endocrinol* 8, 81.

Conkright, M.D., Canettieri, G., Screaton, R., Guzman, E., Miraglia, L., Hogenesch, J.B. and Montminy, M. (2003) TORCs: transducers of regulated CREB activity. *Molecular Cell* 12, 413-423.

Corrado, A., Sanpaolo, E.R., Di Bello, S. and Cantatore, F.P. (2017) Osteoblast as a target of anti-osteoporotic treatment. *J Postgrad Med* 129, 858-865.

Datta, N.S. and Abou-Samra, A.B. (2009) PTH and PTHrP signaling in osteoblasts. *Cell Signal* 21, 1245-1254.

Doorn, J., Siddappa, R., Blitterswijk, C.A.v. and Boer, J.d. (2012) Forskolin enhances in vivo bone formation by human mesenchymal stromal cells. *Tissue Engineering Part*

A 18, 558-567.

Du, W.Q., Zheng, J.N. and Pei, D.S. (2016) The diverse oncogenic and tumor suppressor roles of salt-inducible kinase (SIK) in cancer. *Expert Opin Ther Targets* 20, 477-485.

Gallo, E.F. and Iadecola, C. (2011) Balancing Life and Death in the Ischemic Brain: SIK and TORC Weigh In. *Neuron* 69, 3-6.

Ge, C.X., Yang, Q., Zhao, G.S., Yu, H., Kirkwood, K.L. and Franceschi, R.T. (2012) Interactions between extracellular signal-regulated kinase 1/2 and P38 Map kinase pathways in the control of RUNX2 phosphorylation and transcriptional activity. *J Bone Miner Res* 27, 538-551.

Gonzalez, G.A. and Montminy, M.R. (1989) Cyclic AMP stimulates somatostatin gene transcription by phosphorylation of CREB at serine 133. *Cell* 59, 675-680.

Greenblatt, M.B., Shim, J.H., Zou, W.G., Sitara, D., Schweitzer, M., Hu, D., Lotinun, S., Sano, Y., Baron, R., Park, J.M., et al. (2010) The p38 MAPK pathway is essential for skeletogenesis and bone homeostasis in mice. *J Clin Invest* 120, 2457-2473.

Hardie, D.G. and Carling, D. (1997) The AMP-activated protein kinase--fuel gauge of the mammalian cell? *Eur J Biochem* 246, 259-273.

Hayashi, M., Nimura, K., Kashiwagi, K., Harada, T., Takaoka, K., Kato, H., Tamai, K. and Kaneda, Y. (2007) Comparative roles of Twist-1 and Id1 in transcriptional regulation by BMP signaling. *J Cell Sci* 120, 1350-1357.

Henriksson, E., Jones, H.A., Patel, K., Peggie, M., Morrice, N., Sakamoto, K. and Goransson, O. (2012) The AMPK-related kinase SIK2 is regulated by cAMP via phosphorylation at Ser(358) in adipocytes. *Biochem J* 444, 503-514.

Huang, W., Yang, S., Shao, J. and Li, Y.-P. (2007) Signaling and transcriptional regulation in osteoblast commitment and differentiation. *Front Biosci* 12, 3068-3092.

Jaleel, M., McBride, A., Lizcano, J.M., Deak, M., Toth, R., Morrice, N.A. and Alessi, D.R. (2005) Identification of the sucrose non-fermenting related kinase SNRK, as a novel LKB1 substrate. *FEBS Lett* 579, 1417-1423.

Jongen, J.W., Bos, M.P., van der Meer, J.M. and Herrmann-Erlee, M.P. (1993) Parathyroid hormone-induced changes in alkaline phosphatase expression in fetal

calvarial osteoblasts: differences between rat and mouse. *J Cell Physiol* 155, 36-43.

Katagiri, T., Yamaguchi, A., Ikeda, T., Yoshiki, S., Wozney, J.M., Rosen, V., Wang, E.A., Tanaka, H., Omura, S. and Suda, T. (1990) The non-osteogenic mouse pluripotent cell line, C3H10T1/2, is induced to differentiate into osteoblastic cells by recombinant human bone morphogenetic protein-2. *Biochem Biophys Res Commun* 172, 295-299.

Katagiri, T., Yamaguchi, A., Komaki, M., Abe, E., Takahashi, N., Ikeda, T., Rosen, V., Wozney, J.M., Fujisawa-Sehara, A. and Suda, T. (1994) Bone morphogenetic protein-2 converts the differentiation pathway of C2C12 myoblasts into the osteoblast lineage. *J Cell Biol* 127, 1755-1766.

Katoh, Y., Takemori, H., Lin, X.Z., Tamura, M., Muraoka, M., Satoh, T., Tsuchiya, Y., Min, L., Doi, J., Miyauchi, A., et al. (2006) Silencing the constitutive active transcription factor CREB by the LKB1-SIK signaling cascade. *FEBS J* 273, 2730-2748.

Kennel, K.A. and Drake, M.T. (2009) Adverse effects of bisphosphonates: implications for osteoporosis management. *Mayo Clin Proc* 84, 632-637; quiz 638.

Kim, H., Lee, Y.D., Kim, M.K., Kwon, J.O., Song, M.K., Lee, Z.H. and Kim, H.H. (2017) Extracellular S100A4 negatively regulates osteoblast function by activating the NF-kappaB pathway. *BMB Rep* 50, 97-102.

Kim, H.J., Prasad, V., Hyung, S.W., Lee, Z.H., Lee, S.W., Bhargava, A., Pearce, D., Lee, Y. and Kim, H.H. (2012) Plasma membrane calcium ATPase regulates bone mass by fine-tuning osteoclast differentiation and survival. *J Cell Biol* 199, 1145-1158.

Kim, J.M., Choi, J.S., Kim, Y.H., Jin, S.H., Lim, S., Jang, H.J., Kim, K.T., Ryu, S.H. and Suh, P.G. (2013) An activator of the cAMP/PKA/CREB pathway promotes osteogenesis from human mesenchymal stem cells. *J Cell Physiol* 228, 617-626.

Kim, M.J., Park, S.K., Lee, J.H., Jung, C.Y., Sung, D.J., Park, J.H., Yoon, Y.S., Park, J., Park, K.G., Song, D.K., et al. (2015) Salt-Inducible Kinase 1 terminates cAMP signaling by an evolutionarily conserved negative-feedback loop in beta-cells. *Diabetes* 64, 3189-3202.

Kondo, H., Ohyama, T., Ohya, K. and Kasugai, S. (1997) Temporal changes of mRNA expression of matrix proteins and parathyroid hormone and parathyroid hormone-related protein (PTH/PTHrP) receptor in bone development. *J Bone Miner Res* 12, 2089-2097.

Korchynskyi, O. and ten Dijke, P. (2002) Identification and functional characterization of distinct critically important bone morphogenetic protein-specific response elements in the Id1 promoter. *J Biol Chem* 277, 4883-4891.

Lee, K.S., Hong, S.H. and Bae, S.C. (2002) Both the Smad and p38 MAPK pathways play a crucial role in Runx2 expression following induction by transforming growth factor-beta and bone morphogenetic protein. *Oncogene* 21, 7156-7163.

Li, S., Zhang, C., Takemori, H., Zhou, Y. and Xiong, Z.-Q. (2009) TORC1 regulates activity-dependent CREB-target gene transcription and dendritic growth of developing cortical neurons. *J Neurosci* 29, 2334-2343.

Lin, R.Z., Chen, J., Hu, Z.W. and Hoffman, B.B. (1998) Phosphorylation of the cAMP response element-binding protein and activation of transcription by alpha1 adrenergic receptors. *J Biol Chem* 273, 30033-30038.

Lizcano, J.M., Göransson, O., Toth, R., Deak, M., Morrice, N.A., Boudeau, J., Hawley, S.A., Udd, L., Mäkelä, T.P., Hardie, D.G., et al. (2004) LKB1 is a master kinase that activates 13 kinases of the AMPK subfamily, including MARK/PAR-1. *EMBO J* 23, 833-843.

Lombardi, M.S., Gilliéron, C., Berkelaar, M. and Gabay, C. (2017) Salt-inducible kinases (SIK) inhibition reduces RANKL-induced osteoclastogenesis. *PLOS ONE* 12, e0185426.

Lombardi, M.S., Gillieron, C., Dietrich, D. and Gabay, C. (2016) SIK inhibition in human myeloid cells modulates TLR and IL-1R signaling and induces an anti-inflammatory phenotype. *J Leukoc Biol* 99, 711-721.

Long, F. (2011) Building strong bones: molecular regulation of the osteoblast lineage. *Nat Rev Mol Cell Biol* 13, 27.

Lopez-Rovira, T., Chalaux, E., Massague, J., Rosa, J.L. and Ventura, F. (2002) Direct binding of Smad1 and Smad4 to two distinct motifs mediates bone morphogenetic protein-specific transcriptional activation of Id1 gene. *J Biol Chem* 277, 3176-3185.

Lotinun, S., Sibonga, J.D. and Turner, R.T. (2002) Differential effects of intermittent and continuous administration of parathyroid hormone on bone histomorphometry and gene expression. *Endocrine* 17, 29-36.

Maeda, Y., Tsuji, K., Nifuji, A. and Noda, M. (2004) Inhibitory helix-loop-helix transcription factors Id1/Id3 promote bone formation in vivo. *J Cell Biochem* 93, 337-344.

Martinkovich, S., Shah, D., Planey, S.L. and Arnott, J.A. (2014) Selective estrogen receptor modulators: tissue specificity and clinical utility. *Clin Interv Aging* 9, 1437-1452.

Meyer, L. (2019) FDA approves new treatment for osteoporosis in postmenopausal women at high risk of fracture. *www.fda.gov*.

Miyazono, K., Maeda, S. and Imamura, T. (2005) BMP receptor signaling: Transcriptional targets, regulation of signals, and signaling cross-talk. *Cytokine Growth Factor Rev* 16, 251-263.

Miyazono, K. and Miyazawa, K. (2002) Id: a target of BMP signaling. *Science's STKE* 2002, pe40-pe40.

Nixon, M., Stewart-Fitzgibbon, R., Fu, J., Akhmedov, D., Rajendran, K., Mendoza-Rodriguez, M.G., Rivera-Molina, Y.A., Gibson, M., Berglund, E.D., Justice, N.J., et al. (2016) Skeletal muscle salt inducible kinase 1 promotes insulin resistance in obesity. *Molecular Metabolism* 5, 34-46.

Ogata, T., Wozney, J.M., Benezra, R. and Noda, M. (1993) Bone morphogenetic protein 2 transiently enhances expression of a gene, Id (inhibitor of differentiation), encoding a helix-loop-helix molecule in osteoblast-like cells. *Proc Natl Acad Sci U S A* 90, 9219-9222.

Oh, J.E., Kim, H.J., Kim, W.S., Lee, Z.H., Ryoo, H.M., Hwang, S.J., Lee, Y. and Kim, H.H. (2012) PlexinA2 mediates osteoblast differentiation via regulation of Runx2. *J Bone Miner Res* 27, 552-562.

Ohta, Y., Nakagawa, K., Imai, Y., Katagiri, T., Koike, T. and Takaoka, K. (2008) Cyclic AMP enhances Smad-mediated BMP signaling through PKA-CREB pathway. *J Bone Miner Metab* 26, 478-484.

Okamoto, M., Takemori, H. and Katoh, Y. (2004) Salt-inducible kinase in steroidogenesis and adipogenesis. *Trends Endocrinol Metab* 15, 21-26.

Park, J., Yoon, Y.S., Han, H.S., Kim, Y.H., Ogawa, Y., Park, K.G., Lee, C.H., Kim, S.T. and Koo, S.H. (2014) SIK2 is critical in the regulation of lipid homeostasis and adipogenesis in vivo. *Diabetes* 63, 3659-3673.

Peng, Y., Kang, Q., Luo, Q., Jiang, W., Si, W., Liu, B.A., Luu, H.H., Park, J.K., Li, X., Luo, J., et al. (2004) Inhibitor of DNA binding/differentiation helix-loop-helix proteins mediate bone morphogenetic protein-induced osteoblast differentiation of mesenchymal stem cells. *J Cell Biochem* 279, 32941-32949.

Rutkovskiy, A., Stenslokken, K.O. and Vaage, I.J. (2016) Osteoblast Differentiation at a Glance. *Med Sci Monit Basic Res* 22, 95-106.

Sall, J., Pettersson, A.M., Bjork, C., Henriksson, E., Wasserstrom, S., Linder, W., Zhou, Y., Hansson, O., Andersson, D.P., Ekelund, M., et al. (2017) Salt-inducible kinase 2 and -3 are downregulated in adipose tissue from obese or insulin-resistant individuals: implications for insulin signalling and glucose uptake in human adipocytes. *Diabetologia* 60, 314-323.

Sanosaka, M., Fujimoto, M., Ohkawara, T., Nagatake, T., Itoh, Y., Kagawa, M., Kumagai, A., Fuchino, H., Kunisawa, J., Naka, T., et al. (2015) Salt-inducible kinase 3 deficiency exacerbates lipopolysaccharide-induced endotoxin shock accompanied by increased levels of pro-inflammatory molecules in mice. *Immunology* 145, 268-278.

Sasagawa, S., Takemori, H., Uebi, T., Ikegami, D., Hiramatsu, K., Ikegawa, S., Yoshikawa, H. and Tsumaki, N. (2012) SIK3 is essential for chondrocyte hypertrophy during skeletal development in mice. *Development* 139, 1153-1163.

Scobey, M.J., Fix, C.A. and Walker, W.H. (2004) The Id2 transcriptional repressor is induced by follicle-stimulating hormone and cAMP. *J Biol Chem* 279, 16064-16070.

Screaton, R.A., Conkright, M.D., Katoh, Y., Best, J.L., Canettieri, G., Jeffries, S., Guzman, E., Niessen, S., Yates, J.R., Takemori, H., et al. (2004) The CREB coactivator TORC2 functions as a calcium- and cAMP-sensitive coincidence detector. *Cell* 119, 61-74.

Siddappa, R., Martens, A., Doorn, J., Leusink, A., Olivo, C., Licht, R., van Rijn, L., Gaspar, C., Fodde, R., Janssen, F., et al. (2008) cAMP/PKA pathway activation in human mesenchymal stem cells in vitro results in robust bone formation in vivo. *Proc Natl Acad Sci U S A* 105, 7281-7286.

Sonntag, T., Vaughan, J.M. and Montminy, M. (2018) 14-3-3 proteins mediate inhibitory effects of cAMP on salt-inducible kinases (SIKs). *FEBS J* 285, 467-480.

Stewart, R., Akhmedov, D., Robb, C., Leiter, C. and Berdeaux, R. (2013) Regulation of SIK1 abundance and stability is critical for myogenesis. *Proc Natl Acad Sci U S A* 110,

117-122.

Takayanagi, H., Kim, S., Koga, T., Nishina, H., Isshiki, M., Yoshida, H., Saiura, A., Isobe, M., Yokochi, T., Inoue, J., et al. (2002) Induction and activation of the transcription factor NFATc1 (NFAT2) integrate RANKL signaling in terminal differentiation of osteoclasts. *Dev Cell* 3, 889-901.

Takemori, H., Doi, J., Horike, N., Katoh, Y., Min, L., Lin, X.-z., Wang, Z.-n., Muraoka, M. and Okamoto, M. (2003) Salt-inducible kinase-mediated regulation of steroidogenesis at the early stage of ACTH-stimulation. *J Steroid Biochem Mol Biol* 85, 397-400.

Takemori, H., Kajimura, J. and Okamoto, M. (2007) TORC□SIK cascade regulates CREB activity through the basic leucine zipper domain. *FEBS J* 274, 3202-3209.

Takemori, H., Katoh, Y., Horike, N., Doi, J. and Okamoto, M. (2002) ACTH-induced nucleocytoplasmic translocation of salt-inducible kinase: Impication in the protein kinase A-activated gene transcription in mouse adrenocortical tumor cells. *J Biol Chem* 277, 42334-42343.

Tare, R.S., Oreffo, R.O., Clarke, N.M. and Roach, H.I. (2002) Pleiotrophin/osteoblast-stimulating factor 1: dissecting its diverse functions in bone formation. *J Bone Miner Res* 17, 2009-2020.

Taub, M., Springate, J.E. and Cutuli, F. (2010) Targeting of renal proximal tubule Na,K-ATPase by salt-inducible kinase. *Biochem Biophys Res Commun* 393, 339-344.

Traianedes, K., Dallas, M.R., Garrett, I.R., Mundy, G.R. and Bonewald, L.F. (1998) 5-Lipoxygenase metabolites inhibit bone formation in vitro. *Endocrinology* 139, 3178-3184.

van der Linden, A.M., Nolan, K.M. and Sengupta, P. (2007) KIN□29 SIK regulates chemoreceptor gene expression via an MEF2 transcription factor and a class II HDAC. *EMBO J* 26, 358-370.

Viale-Bouroncle, S., Klingelhoffer, C., Ettl, T., Reichert, T.E. and Morsczeck, C. (2015) A protein kinase A (PKA)/beta-catenin pathway sustains the BMP2/DLX3-induced osteogenic differentiation in dental follicle cells (DFCs). *Cell Signal* 27, 598-605.

Vilardaga, J.-P., Romero, G., Friedman, P.A. and Gardella, T.J. (2011) Molecular basis of parathyroid hormone receptor signaling and trafficking: a family B GPCR paradigm. *Cell Mol Life Sci* 68, 1-13.

Wein, M.N., Foretz, M., Fisher, D.E., Xavier, R.J. and Kronenberg, H.M. (2018) Salt-inducible kinases: physiology, regulation by cAMP, and therapeutic potential. *Trends Endocrin Met* 29, 723-735.

Wein, M.N., Liang, Y., Goransson, O., Sundberg, T.B., Wang, J., Williams, E.A., O'Meara, M.J., Govea, N., Beqo, B., Nishimori, S., et al. (2016) SIKs control osteocyte responses to parathyroid hormone. *Nat Commun* 7, 13176.

Wu, M., Chen, G. and Li, Y.-P. (2016) TGF-β and BMP signaling in osteoblast, skeletal development, and bone formation, homeostasis and disease. *Bone Res* 4, 16009.

Yang, R. and Gerstenfeld, L.C. (1996) Signal transduction pathways mediating parathyroid hormone stimulation of bone sialoprotein gene expression in osteoblasts. *J Biol Chem* 271, 29839-29846.

Yong Kim, S., Jeong, S., Chah, K.-H., Jung, E., Baek, K.-H., Kim, S.-T., Shim, J.-H., Chun, E. and Lee, K.-Y. (2013) Salt-Inducible Kinases 1 and 3 negatively regulate toll-like receptor 4-mediated signal. *Mol Endocrinol* 27, 1958-1968.

Yoon, S.H., Ryu, J., Lee, Y., Lee, Z.H. and Kim, H.H. (2011) Adenylate cyclase and calmodulin-dependent kinase have opposite effects on osteoclastogenesis by regulating the PKA-NFATc1 pathway. *J Bone Miner Res* 26, 1217-1229.

Zaheer, S., LeBoff, M. and Lewiecki, E.M. (2015) Denosumab for the treatment of osteoporosis. *Expert Opin Drug Metab Toxicol* 11, 461-470.

Zhang, H., Li, L., Dong, Q., Wang, Y., Feng, Q., Ou, X., Zhou, P., He, T. and Luo, J. (2015) Activation of PKA/CREB signaling is involved in BMP9-induced osteogenic differentiation of mesenchymal stem cells. *Cell Physiol Biochem* 37, 548-562.

Zhao, L., Yang, S., Zhou, G.Q., Yang, J., Ji, D., Sabatakos, G. and Zhu, T. (2006) Downregulation of cAMP-dependent protein kinase inhibitor gamma is required for BMP-2-induced osteoblastic differentiation. *Int J Biochem Cell Biol* 38, 2064-2073.

Zhao, M., Edwards, J., Ko, S., Parlato, R., Harris, S. and Mundy, G. (2009) CREB induces BMP2 transcription in osteoblasts and CREB knockout reduces bone mass in mice. *Bone* 44, S27.

국문초록

Salt-inducible kinase 1의 CRTC1을 통한 조골세포 분화 조절

서울대학교 대학원 세포및발생생물학 전공

(지도교수: 김홍희)

김민경

골대사과정의 여러 단계를 조절하는 분자 및 세포 수준의 기작을 잘 이해하는 것이 골다공증 같은 골 질환을 예방하거나 치료하는 치료 물질의 개발에 중요하다. 본 연구는 조골세포의 분화를 조절하는데

있어서의 salt-inducible kinase 1 (SIK1)의 역할을 규명하였다. 특히, 조골세포 분화과정에서 SIK 동형 족 중의 SIK1 발현이 현저하게 감소되었다. 조골전구세포에서 SIK2와 SIK3의 유전자와는 다르게, SIK1의 유전자 발현이 낮아질 때 조골세포의 분화와 석회화가 촉진되었다. 뿐만 아니라, SIK1은 조골전구세포의 증식도 조절하였다. 또한 SIK1 효소 활성이 조골세포 분화를 조절하는데 필요함을 밝혔다. SIK1은 CREB regulated transcription coactivator 1 (CRTC1)을 인산화하여, CREB 전사작용을 억제함으로써, Id1과 같은 골 동화작용 유전자의 발현을 저해하였다. SIK1 유전자가 결여된 마우스는 야생형 마우스에 비해 골량, 조골세포의 수, 골 형성율 등 골 동화의 기준척도의 증가를 보였다. 반면, SIK1 유전자가 결여된 마우스와 야생형 마우스 사이에서 파골세포의 수와 RANKL/OPG 비율에는 차이가 없었다. 더불어, bone morphogenic protein 2 (BMP2)가 SIK1 발현과 효소활성을 protein kinase

A (PKA) 의존적인 방식으로 감소시킨다는 사실을 밝혔다. 종합해보면, 본 연구 결과는 SIK1이 CRTC1/CREB 축을 통해 조골전구세포의 증식과 조골세포의 분화에 중요한 역할을 한다는 것과 SIK1의 억제가 골동화과정 동안 BMP2 신호전달에 중요하다는 것을 증명한다. 따라서, SIK1의 골 질환에 대한 치료약의 분자 후보로서의 활용 가능성이 제시된다.

주요어: 조골세포, SIK1, BMP2, CRTC1, CREB, Id1, PKA

학번: 2012-21832

이 학위논문은 “Cell Death and Disease” 학술지에 출판된 연구결과를

포함하고 있다.